Analysis of Piezoelectric Energy Harvesting for Bridge Health Monitoring Systems

Author: Amin Mohammad Hedayetullah

Student ID: 530185

Supervised By: Prof. Sondipon Adhikari & Prof. M.I. Friswell

Date of submission: 3rd June 2010

Swansea University
Prifysgol Abertawe

"Project Dissertation submitted to the University of Wales Swansea in Partial Fulfilment for the Degree of Erasmus Mundus Master of Science in Computational Mechanics"

Civil and Computational Engineering Centre, School of Engineering

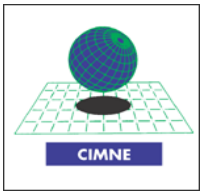

Declaration

- This work has not previously been accepted in substance for any degree and is not being currently submitted in candidature for any degree.
- This dissertation is being submitted in partial fulfilment of the requirements for the degree of MSc.
- This dissertation is the result of my own independent work/investigation, except where otherwise stated. Other sources are acknowledged by giving explicit references. A bibliography is appended.
- I hereby give consent for my dissertation, if accepted, to be available for photocopying and for inter-library loan, and for the title and summary to be made available to outside organisations.

.....
Amin Mohammad Hedayetullah
03/06/2010

Acknowledgement

No journey is fulfilled without the companions. For me, my journey was more complicated as the first few steps are always difficult in the world of research for any new researcher. It was my supervisors,Prof. Sondipon Adhikari and Prof. M.I. Friswell, who never let me went alone in those early daunting days. No word is sufficient to thank them for their enormous support,mentoring throughout this venture.Special thanks to my course co ordinator, Dr. A.I.J. Gil for his advice and guidence during the whole course curriculum.

I would like to thank my parents, they are the one for whom I am here now. I am also greatful to my friends and colleagues for their all around cooperation.

Last but not the least, the Erasmus Mundus Scheme Authority for providing us with such an excellent opprtunity to explore the engineering arena of modern world.

Contents

List of Figures

List of Tables

Abstract

Energy harvesting (also known as power harvesting or energy scavenging) is the process by which energy is derived from external sources (e.g., solar power, thermal energy, wind energy, salinity gradients, and kinetic energy), captured, and stored.In the last few years, there has been a surge of research in the area of power harvesting. This increase in research has been brought on by the modern advances in wireless technology and low power electronics such as micro-electromechanical systems (MEMS). The advances have allowed numerous doors to open for power harvesting systems in practical real world applications e.g. small scale wireless sytems.On the other hand, wireless sensor systems, in Structural Health Monitoring(SHM) context, are receiving increasing interest since they offer flexibility, ease of implementation and the ability to retrofit systems without the cost and inconvenience of cabling. Furthermore, by removing wires there is the potential for embedding sensors in previously inaccessible locations. At present, the majority of wireless sensor nodes are simply battery-powered which need periodic replacement. If ambient energy in the surrounding medium could be obtained, then it could be used to replace or charge the battery. One method is to use piezoelectric materials to obtain energy lost due to vibrations of the host structure. This captured energy could then be used to prolong the life of the power supply or in the ideal case provide endless energy for the electronic devices lifespan. From previous work it is evident that the power generated by the piezoelectric devices was sufficient for powering functional wireless devices.But these are focused basically on the vibration of the industrial machines i.e. harmonic vibration as a source . On the other hand, energy harvesters used in the bridge health monitoring is based on electromagnetism concept rather than utilizing piezoelectricity. So, a combination of piezoelectric energy harvester along with vibration of the bridge under traffic movement worth attention. On top of this, the derived concepts can be adopted to many other fields which might trigger enormous filed of opportunities.

Chapter 1

Inroduction

1.1 Structural Health Monitoring System

Structures, including bridges, buildings, dams, pipelines, aircraft, ships, among others, are complex engineered systems that ensure society's economic and industrial prosperity. To design structures that are safe for public use, standardized building codes and design methodologies have been created. Unfortunately, structures are often subjected to harsh loading scenarios and severe environmental conditions not anticipated during design that will result in long-term structural deterioration.To design safer and more durable structures, the engineering community is aggressively pursuing novel sensing technologies and analytical methods that can be used to rapidly identify the onset of structural damage in an instrumented structural system. Called structural health monitoring (SHM), this offers an automated method for tracking the health of a structure by combining damage detection algorithms with structural monitoring systems.

1.2 Wireless Monitoring System

The monitoring system is primarily responsible for collecting the measurement output from sensors installed in the structure and storing the measurement data within a central data repository. To guarantee that measurement data are reliably collected, structural monitoring systems employ coaxial wires for communication between sensors and the repository. While coaxial wires provide a very reliable communication link, their installation in structures can be expensive and labour-intensive[18].For example, it was reported that a SHM system installed in a tall buildings generally cost in excess of $US5000 per sensing channel [4]. As SHM systems grow in size (as defined by the total number of sensors), to assess the current status of the structure accurately, the cost of the monitoring system can grow much faster than at a linear rate. For example, the cost of installing about 350 sensing channels on Tsing Ma Suspension Bridge in Hong Kong was estimated to have exceeded $8 million [5]. If the maintenance cost of the SHM system, which will be increased as the system gets older, is also considered, the total cost may be increased exponentially. This limitation on economical realization of SHM system may prevent installation of large number of sensors enough to assess the accurate status of a large civil structure, if the big budget for the SHM system is not secured.So,Wireless sensor systems are receiving increasing interest since they offer flexibility, ease of implementation and the ability to retrofit systems without the cost and inconvenience of cabling.Smart wireless sensor is an emerging sensor with the following essential features: on-board

micro-processor, sensing capability, wireless communication, battery powered, and low cost [5]. When many sensors are implemented on a SHM system for a sizable civil structure, wireless communication between sensors and data repository seems to be attractive in the aspects of the cost. Dense arrays of low-cost smart wireless sensors have the potential to improve the quality of the SHM dramatically using their onboard computational and wireless communication capabilities. These wireless sensors provide rich information which SHM algorithms can utilize to detect, locate, and assess structural damage caused by severe loading events and by progressive environmental deterioration as well as economical realization of SHM system. Information from densely instrumented structures is expected to result in the deeper insight into the physical state of the structural system. Furthermore, by removing wires there is the potential for embedding sensors in previously inaccessible locations.An overview of the idea is presented in the Figure 1.1

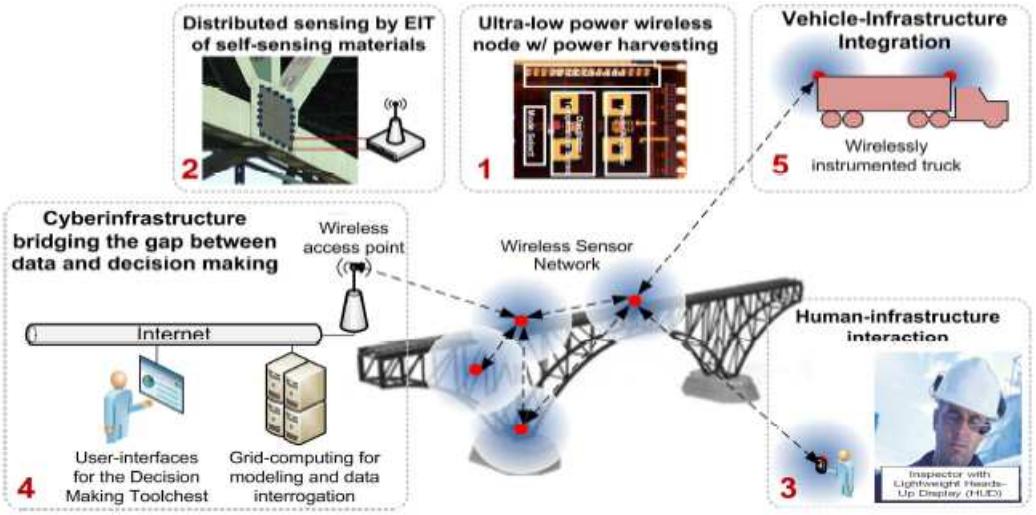

Figure 1.1: Wireless bridge monitoring system overview[22]

1.2.1 Power Consumption for SHM sensors

A monitoring system is supposed to work for a longer period that means for several month or years. A detailed bridge inspection will take place at an interval of three or six years in for example. It is therefore desired, that the life time of the monitoring system is also three years at least.

An important aspect in designing and in programming a sensor node is to minimize its overall power consumption. As a first step it is recommended to look for an optimized hardware. There are a lot of power consuming components like the sensors, the A/D-conversion-module, the radio module, the sensor- CPU, and the memory which require energy to work properly (1.1). If low power consumption is considered it is suggested to limit the voltage range of these components to a maximum value of 5 Volt or better of about 3 Volt or even lower.

In a next step it is recommended that the system components operate in sleep or power down mode as often as possible. These modes require only little energy. Most of the used radio modules and processors support such power saving modes. Some of the devices could also be switched off if not needed. For this reason a monitoring system has to provide different event handling and wake up modes. Hard- and software has to be optimized in this way.

Another high power consuming part is represented by the sampling rate and the amount of handled data, e.g. high sampling rates and high amplitude resolution result in high power consumption.

In fact power consumption of temperature or humidity measurements is not a problem. Moreover it becomes of interest to monitor dynamic behaviour or uses acoustic emission techniques with high sampling rates.

Table 1.1: Average energy required for different components (at 3V)[31]

Component	Sleep mode	Full Operation
8-bit processor at 20 MHz	24μW	24mW
Memory	6μW	45mW(writing)
		12mW(reading)
Radio Module(RF)	6μW	24mW (receiving)
		36mW (trasmmitting)
Signal Conditioning and A/D Conversion		
100KHz, 12bit		0.6to12mW
MEMS Sensors		
Acceleration 2KHz,12 bit	15μW	6 to 15 mW
Humidity and Temperature	$1\mu W$	1.5mW

Nowadays battery powered systems, e.g. equipped with Lithium-batteries, are most appropriate. However, power supplies like solar cells, methanol powered fuel cells are alternatives. Ongoing research is made in the field of energy harvesting, for example for cellular phones.

1.2.2 Wireless Communication

It is suggested that for most monitoring tasks a communication range of 10 to 30 m is sufficient. There are some communication standards like WLAN (IEEE802.11, wireless local area network) and Bluetooth that are well known and feature such ranges. Different famous wireless communication systems' power requirement is presented in the table(1.2)

Table 1.2: Average energy required per transmitted bit and maximum data transfer rate[31]

Communication standard	12 m distance	30 m distance	Max. Transfer rate
IEEE 802.11b (WLAN)	200 nJ/bit	300 nJ/bit	11 Mbps
Bluetooth	2.5 µJ/bit		0.8 Mbps
Zigbee	7 µJ/bit	7 µJ/bit	20 to 250 kbps
Home-RF (example)	1 µJ/bit	2 µJ/bit	0.8 to 2 Mbps
nanoNET (CSS)	60 nJ/bit	80 nJ/bit	2 Mbps

With regard to the power consumption of the different communication methods for saving energy it is suggested to send relevant data to other sensor nodes or the central unit only, because signal processing in the sensor node needs less power than sending it through the radio module.

1.3 Energy Harvesting for Sensors

Harvesting ambient energy, for example from mechanical vibrations, is very attractive for wireless autonomous sensor networks[17]. From previous work it is evident that the power generated by the piezoelectric devices was sufficient for powering functional wireless devices and were able to transmit a 12-bit signal five to six times every few seconds[3]. Another investigation features a foot print of $1cm^2$ and an average power harvesting level of $100\mu W$[17].Additionally, it is also very important for systems which do not allow battery replacement or are not able to have wired power coupling.

Furthermore, these devices have to be relatively small in order to be applicable in autonomous wireless transducer systems.Energy harvesting can be performed e.g. by mechanical energy conversion based on piezoelectric, electrostatic and electromagnetic principles or by employing thermoelectric generation exploiting a temperature gradient [17].

Many industrial and automotive environments provide vibration frequencies ranging from a few tens of Hz up to several kHz. Normally this energy remains unused or is even dissipated in mechanical dampers. Vibrational energy harvesters tap into this energy reservoir. The ambient vibration is used to excite a mechanical resonator consisting of a spring suspended seismic mass. The amplitude of the mass under resonant excitation is used to drive an energy conversion mechanism. The most common ones are: piezoelectric, electrostatic and electromagnetic principles. The first principle received the most attention due to its ability to directly convert mechanical strain into electrical energy at usable voltage levels[17].

1.3.1 Electrostatic Vibration Energy Harvesting

The first mechanism of conversion is based on the variable capacitor concept. A variable capacitor consists of two conductors separated by a dielectric material. When the conductors are placed in an electric field and the conductors are moved relative to each other, current is generated[27].

Figure 1.2 shows two possible implementations of such a variable capacitor. A seismic mass is suspended via spring elements. In-plane vibration excites considerable displacement of the electrodes and thus leads to a usable change in capacitance. So far, several silicon micro structures have been proposed which realize variable capacitors. Either they provide linear capacitance change with displacement [10, 11, 13] or non-linear variation [12, 14, 8, 7]. The first case uses varying overlap of two parallel electrodes, while the second approach uses the increase in capacitance as the spacing between two parallel electrodes is reduced.

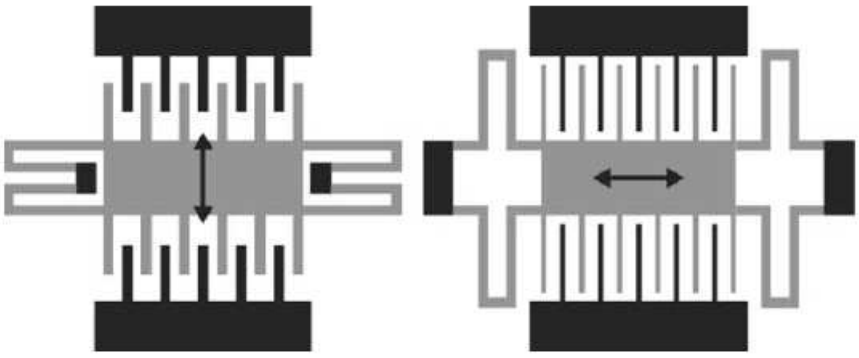

Figure 1.2: Implementation of electrostatic energy harvesters. Left: linearly changing capacitance due to change in electrode overlap, right: non-linear change in capacitance due to change in electrode spacing[17]

The design as shown in Figure 1.3 implements a varying overlap capacitor. The lower set of electrodes is recessed in a substrate while the movable electrodes are connected to the seismic mass.

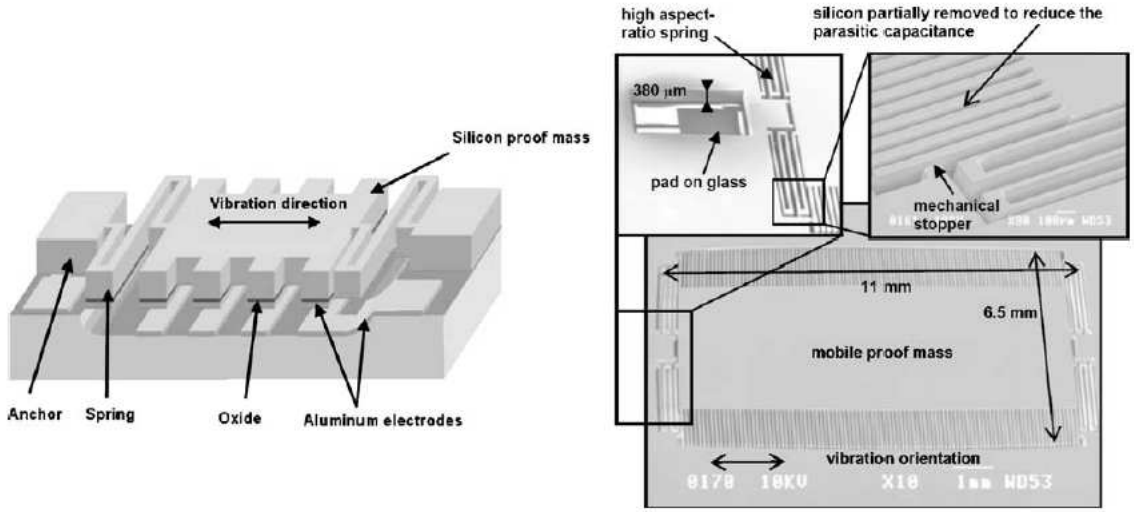

Figure 1.3: Design of a variable overlap capacitor and fabricated silicon micro structure. The capacitor electrodes are fabricated on the substrate and on the movable mass. Displacement of the mass results in a change in overlap and decreases the capacitance consecutively[7]

The design as shown in Figure 1.4 implements a varying gap capacitor. Here, the electrodes are perpendicular to the substrate plane. Mechanical switches (SW1 and SW2) are integrated with the structure to synchronize the charge transfer with the motion of the mass.

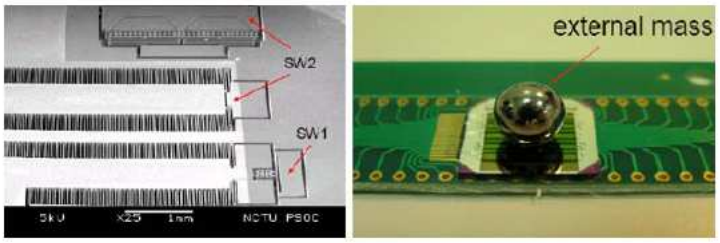

Figure 1.4: A mechanical resonator using capacitor structures with varying gap . The arrangement of interdigitating fingers can lead to substantial increase of capacitance as the electrodes come close to each other. A metal ball is attached to the silicon micro structure to increase the seismic mass and thus decrease the resonance frequency[15]

1.3.2 Electromagnetic Vibration Energy Harvesting

The magnetic induction transducer is based on Faraday's law. The variation in magnetic flux, Φ_m through an electrical circuit causes an electric field. This flux variation can be realized with a moving magnet whose flux is linked with a fixed coil or with a fixed magnet whose flux is linked with a moving

coil. The first configuration is preferred to the second one because the electrical wires are fixed. As the relevant magnitude here is the magnetic flux through a circuit, the size of the coil is inversely related to the obtained electric field and therefore, to the generated energy. This means that big transducers with large area coils will perform better than smaller transducers, unless a larger time derivative is involved with the small scale generators[20].Figure1.5 presents the concept.

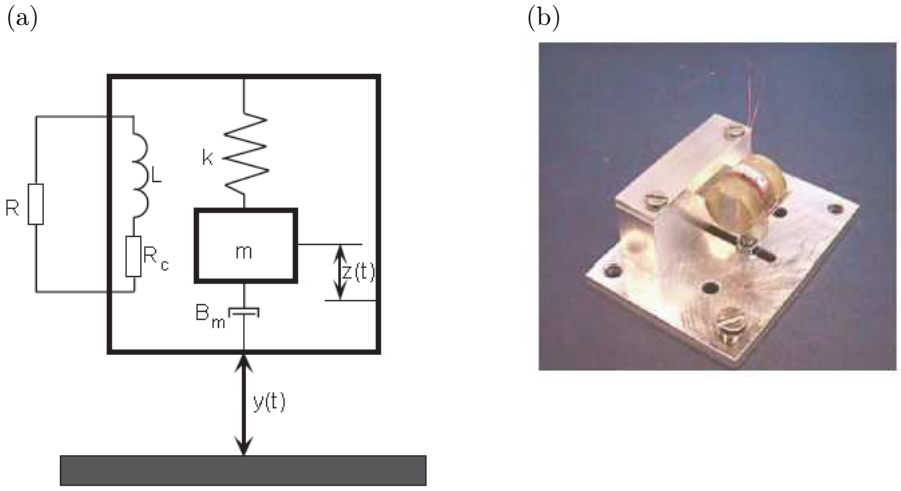

Figure 1.5: (a)Magnetic induction transducer model,(b) A magnetic generator [16]

When the generator vibrates, the oscillating mass has a relative displacement with respect to the housing. The magnetic induction generator converts this relative displacement into electrical energy. The transducer is modelled as a damped spring-mass system, since the energy extraction damps the mass movement with a factor B_m. The mass m, the magnet, which is joined to a spring with a spring constant k moves through a constant magnetic field, B, when the generator oscillates. The relative displacement, $z(t)$, is related to the voltage across the coil by a first order system . L is the inductance of the coil, R_c is the parasitic resistance of the coil, L is the length of the coil, and R is the load resistance[1][16].

1.3.3 Piezoelectric Energy Harvester

Interest in the application of piezoelectric energy harvesters for converting mechanical energy into electrical energy has increased dramatically in recent years, though the idea is not new.Up to now most piezoelectric energy harvesters use a bi morph beam made from a structural material (e.g. steel or silicon) and a stack, which consists of piezoelectric material between two electrodes. While one end of this beam is clamped, a mass is attached to the free end [23, 24]. The bending of the beam section during displacement of the mass causes mechanical strain in the piezo-patch which leads to the generation of an electrical dipole, respectively a charge on the top and bottom electrodes. This charge is used to dissipate power in an attached resistive load. This approach uses the generation of an electrostatic field perpendicular to the applied strain. The triangle-shaped beam section shown in Figure1.6 was chosen to satisfy the maximum limit of the mechanical strain and to achieve a homogeneous strain distribution along the beam length.

[1]The symbols used in this paragraph are kept same as the original one to be consistent and do not resemble any of the symbols used hereafter

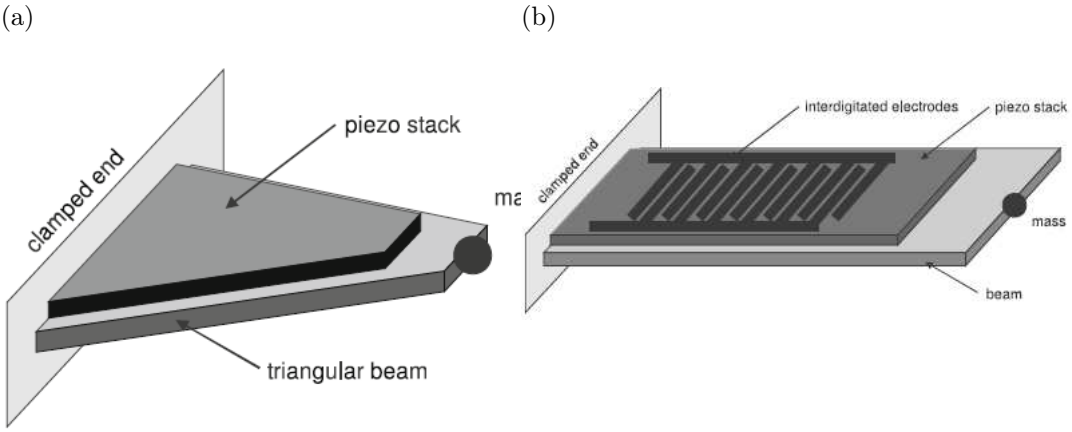

Figure 1.6: Schematic of a piezoelectric energy harvester utilizing (a) the out of-plane dipole generation [17] (b) the inplane dipole generation[17]

The conversion efficiency can even be higher if applied strain and electrical field are in parallel, although in this case the electrode arrangement is not as straight forward as in the previous case. Such a device is described in [21]. Here the electrodes are fabricated as interdigitating fingers, see Figure 1.6(b).

1.4 Scope of the Research

Aiming at a vibration based piezoelectric energy harvester, the scope of the research can be divided into 2 phases:

1. Modeling of the Bridge Dynamics
2. Modeling of the Harvester

Modeling of the Bridge Dynamics consists of considering the Bridge Type and the moving load. The moving load can be also categorized into different types along with the dynamics of the traffic passing through.

Model of the Harvester is basically an Electromechanical Coupled system.So, it has two aspects: designing the mechanical and electrical system.In designing the mechanical system, choosing the proper piezoelectric material(and hence its spring constant and damping ratio) and its mass is the main concern. Also modeling of the damping is another issue.

On the other hand, the electrical part focused on a proper circuit design to get out of the maximum power available from the vibration of the bridge for the sensor.In this case, different circuit parameters as resistance, capacitance etc are key role players.

For the present case, a simple beam with constant moving load is considered in the dynamics part while the electromechanical one is a Single degree of freedom piezoelectric stack with simple Resistance and capacitance.

1.5 Organization of the Thesis

The thesis is organized in the following manner:

Chapter 1,Introduction: The background and motivation of the thesis is explained along with a brief review of some literature. The necessity of doing this thesis topics is posed.Thesis scope and organization are described.

Chapter 2,Bridge Dynamics,Response under constant moving load: A simply supported beam under a constant moving load is considered. Necessary theory both in time and frequency domain are developed elaborately.

Chapter 3, Piezoelectric Energy Harvester: Chapter starts with the piezoelectric basics. With simple explanation constitutive equations for 1D piezoelectric model is developed. At the end, frequency domain solution is obtained.

Chapter 4, Mathematical Modelling and Results: Based on the equations derived in the Chapter 2 and Chapter 3, here a mathematical example is evaluated. Through this the coupled system of bridge dynamics and energy harvester technology are studied.Results are tabulated and plotted.

Chapter 5, Discussion: Explanation of the obtained results.

Chapter 6, Conclusion: Conclusive remarks for the thesis.

Chapter 7, Further Recommendation: Further scope are specified in this chapter.

Chapter 2

Bridge Dynamics: Response Under Constant Moving Load

Of the wide range of problems involving vibration of structures and solids subjected to a moving load, the simplest one to tackle is that of dynamic stresses in a simply supported beam, traversed by a constant force moving at uniform speed. This classical case was first solved by A.N. Krylov, then by S.P. Timoshenko. Other solutions worthy of mention are those by C.E. Inglis and V. Kolousek[1]. In the following sections first the problem is formulated with the necessary assumptions and then solved from two perspectives:(a) Time domain and (b) Frequency domain.

2.1 Formulation of the problem

Let, a constant force P is traversing from left to right on a bridge (modelled as simply supported beam here) of length l at a constant speed c as shown in the Figure 2.1. At any time t, at any point x, measured from the left corner of the bridge, the bridge is deflected $u(x,t)$,measured from the equilibrium position when the beam is loaded with self weight. The bridge is charechterized by the properties as:Young's modulus of the beam,E,constant moment of inertia of the beam cross section ,J,constant mass per unit length of the beam cross section,μ, natural frequency of the beam for nTh mode,ω_n,damping co efficient of the beam for nTh mode,ζ_n

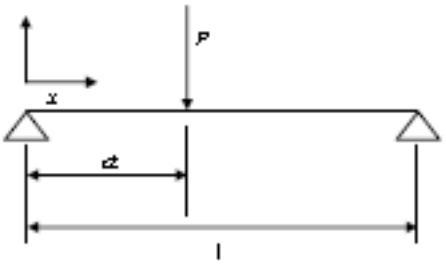

Figure 2.1: Simple beam subjected to a moving force P

Following assumptions[1] are adopted for this case:

1. The beam behaviour is described by Bernoulli-Euler's differential equation deduced on the assumption that the theory of small deformations, Hooke's law, Navier's Hypothesis and Saint-Venant's principle can be applied. The beam is of constant cross-section and constant mass

per unit length.

2. The mass of the moving load is small compared with the mass of the beam; this means that we shall consider only gravitational effects of the load.

3. The load moves at constant speed, from left to right.

4. The beam damping is proportional to the velocity of vibration.

5. The computation will be carried through for a simply supported beam, i.e. a beam with zero deflection and zero bending moment at both ends. Further, at the instant of force arrival, the beam is at rest, i.e. possesses neither deflection nor velocity.

Under the above assumptions the problem is described by the Equation

$$EJ\frac{\partial^4 u(x,t)}{\partial x^4} + \mu\frac{\partial^2 u(x,t)}{\partial t^2} + 2\mu\zeta_n\omega_n\frac{\partial u(x,t)}{\partial t} = \delta(x-ct)P \tag{2.1}$$

The Boundary conditions are
$u(0,t) = 0$;
$u(l,t) = 0$;
At $x = 0, \frac{\partial^2 u(x,t)}{\partial x^2} = 0$;
At $x = l$, $\frac{\partial^2 u(x,t)}{\partial x^2} = 0$;
The Initial Conditions are
$u(x,0) = 0$;
At $t = 0 \frac{\partial u(x,t)}{\partial t}$=0;

2.2 Solution of the problem

Let consider a solution of the problem as

$$u(x,t) = \sum_{n=1}^{\infty} U_n(t)\sin(\frac{n\pi x}{l}) \tag{2.2}$$

Substituting Eq.(2.2) into Eq.(2.1),

$$EJ\sum_{n=1}^{\infty} U_n(t)(\frac{n\pi}{l})^4\sin(\frac{n\pi x}{l}) + \mu\sum_{n=1}^{\infty}\ddot{U}_n(t)\sin(\frac{n\pi x}{l}) + 2\mu\zeta_n\omega_n\sum_{n=1}^{\infty}\dot{U}_n(t)\sin(\frac{n\pi x}{l}) = \delta(x-ct)P \tag{2.3}$$

Multiplying Eq. (2.3)by $\sin(\frac{m\pi x}{l})$ and integrating over an interval 0to$l$,[28]

$$\begin{aligned} EJU_m(t)(\frac{m\pi}{l})^4\frac{l}{2} + \mu\ddot{U}_m(t)\frac{l}{2} + 2\mu\zeta_m\omega_m\dot{U}_m(t)\frac{l}{2} &= \int_0^l \delta(x-ct)P\sin(\frac{m\pi x}{l})dx \\ &= P\sin(\frac{m\pi ct}{l}) \\ &= P\sin(m\Omega t) \end{aligned} \tag{2.4}$$

where, the excitation frequency is given by

$$\Omega = \frac{\pi c}{l} = \frac{\mu}{T}$$

and the natural frequency is given by,

$$\omega_m^2 = \frac{EJ}{\mu}(\frac{m\pi}{l})^4$$

Rearranging Eq.(2.4),

$$\begin{aligned} \ddot{U}_m(t) + 2\zeta_m\omega_m\dot{U}_m(t) + \omega_m^2 U_m(t) &= \frac{Pl}{2\mu}\sin(m\Omega t) \\ &= f_m(t)(\text{Let}) \end{aligned} \tag{2.5}$$

Note that this equation is valid for the time period taken by the force to travel from one end to another end i.e., $0 \leq t \leq T$. For $t \geq T$, i.e. when the force leaves the bridge, there is no forcing function acting on the bridge.Then, the Eq.(2.4) becomes,

$$\ddot{U}_m(t) + 2\zeta_m\omega_m\dot{U}_m(t) + \omega_m^2 U_m(t) = 0 \tag{2.6}$$

2.2.0.1 Frequency Domain Solution

Taking Fourier Transform[28], RHS of the Eq.(2.5) becomes,

$$\begin{aligned} F_m(\omega) &= \frac{1}{\sqrt{2\pi}}\int f_m(t)e^{-j\omega t}dt \\ &= \frac{1}{\sqrt{2\pi}}\int_0^T \frac{Pl}{2\mu}\sin(m\Omega t)e^{-j\omega t}dt \\ &= \frac{1}{\sqrt{2\pi}}\frac{Pl}{2\mu}\int_0^T \frac{1}{2j}(e^{j\omega t} - e^{-j\omega t})e^{-j\omega t}dt \\ &= \frac{1}{\sqrt{2\pi}}\frac{Pl}{2\mu}\frac{1}{2j}\left(\frac{e^{j(m\Omega-\omega)T}}{j(m\Omega-\omega)} + \frac{e^{j(m\Omega-\omega)T}}{j(m\Omega+\omega)} - \frac{1}{j(m\Omega-\omega)} + \frac{1}{j(m\Omega+\omega)}\right) \end{aligned}$$

Taking Laplace Transform[28] of the LHS of the Eq.(2.5), applying boundary conditions and replacing $s = j\omega$gives the Fourier form as,$(-\omega_m^2 + 4j\omega\zeta_m\omega_m + \omega_m^2)U_m(\omega)$.

So, Fourier transform of the Eq.(2.5) gives,

$$U_m(\omega) = \frac{1}{(-\omega_m^2 + 4j\omega\zeta_m\omega_m + \omega_m^2)}\frac{1}{\sqrt{2\pi}}\frac{Pl}{2\mu}\frac{1}{2j}\left(\frac{e^{j(m\Omega-\omega)T}}{j(m\Omega-\omega)} + \frac{e^{j(m\Omega-\omega)T}}{j(m\Omega+\omega)} - \frac{1}{j(m\Omega-\omega)} + \frac{1}{j(m\Omega+\omega)}\right)$$

Replacing $m = n$,

$$U_n(\omega) = \frac{1}{(-\omega_n^2 + 4j\omega\zeta_n\omega_n + \omega_n^2)}\frac{1}{\sqrt{2\pi}}\frac{Pl}{2\mu}\frac{1}{2j}\left(\frac{e^{j(n\Omega-\omega)T}}{j(n\Omega-\omega)} + \frac{e^{j(n\Omega-\omega)T}}{j(n\Omega+\omega)} - \frac{1}{j(n\Omega-\omega)} + \frac{1}{j(n\Omega+\omega)}\right)$$

Thus, taking the Fourier transform of the Eq.(2.2) gives,

$$U(x,\omega) = \sum_{n=1}^{\infty} U_m(\omega)\sin\left(\frac{n\pi x}{l}\right)$$

Frequency Domain solution of the given Eq.(2.1),

$$\begin{aligned} U(x,\omega) &= \sum_{n=1}^{\infty} \frac{1}{(-\omega_n^2 + 4j\omega\zeta_n\omega_n + \omega_n^2)} \frac{1}{\sqrt{2\pi}} \frac{Pl}{2\mu} \frac{1}{2j} * \\ &* \left(\frac{e^{j(n\Omega-\omega)T}}{j(n\Omega-\omega)} + \frac{e^{j(n\Omega-\omega)T}}{j(n\Omega+\omega)} - \frac{1}{j(n\Omega-\omega)} + \frac{1}{j(n\Omega+\omega)} \right) \sin\left(\frac{n\pi x}{l}\right) \end{aligned} \quad (2.7)$$

2.2.0.2 Time Domain Solution

$$\ddot{U}_m(t) + 2\zeta_m\omega_m\dot{U}_m(t) + \omega_m^2 U_m(t) = \frac{Pl}{2\mu}\sin(m\Omega t) \quad (2.8)$$

The complementary (Transient/Homogeneous) solution[28] of Eq.(2.8) is derived from,

$$\ddot{U}_m(t) + 2\zeta_m\omega_m\dot{U}_m(t) + \omega_m^2 U_m(t) = 0 \quad (2.9)$$

Let, the solution of the Eq.(2.9) be,$U_m(t) = ae^{\lambda t}$. So, From Eq.(2.9),

$$(\lambda^2 + 2\zeta_m\omega_m\lambda + \omega_m^2)ae^{\lambda t} = 0$$

The characteristic Equation is given by,

$$(\lambda^2 + 2\zeta_m\omega_m\lambda + \omega_m^2) = 0$$

and therefore,

$$\begin{aligned} \lambda &= -\zeta_m\omega_m + \sqrt{(\zeta_m\omega_m)^2 - \omega_m^2} \\ &= -\omega_b + \sqrt{\omega_b^2 - \omega_m^2} \end{aligned}$$

Replacing, $\zeta_m\omega_m = \omega_b$, where $\omega_b$is the circular frequency of damping of the beam.
The system can be of three types,

1. Over damped, $\omega_b > \omega_m$
2. Critically damped, $\omega_b = \omega_m$
3. Under damped, $\omega_b < \omega_m$

Considering under damped condition,

$$\lambda = -\omega_b \pm j\sqrt{\omega_m^2 - \omega_b^2}$$

Complementary solution

$$\begin{aligned}
U_m^c(t) &= a_1 e^{\lambda_1 t} + a_2 e^{\lambda_2 t} \\
&= a_1 e^{(-\omega_b + j\sqrt{\omega_m^2 - \omega_b^2})t} + a_2 e^{(-\omega_b - j\sqrt{\omega_m^2 - \omega_b^2})t} \\
&= e^{-\omega_b t}\left[(a_1 + a_2)\cos(\sqrt{\omega_m^2 - \omega_b^2})t + (a_1 - a_2)\sin(\sqrt{\omega_m^2 - \omega_b^2})t\right] \\
&= e^{-\omega_b t}\left[A_1 \cos(\sqrt{\omega_m^2 - \omega_b^2})t + A_2 \sin(\sqrt{\omega_m^2 - \omega_b^2})t\right] \\
&= e^{-\omega_b t}\left[A_1 \cos \omega_{dm} t + A_2 \sin \omega_{dm} t\right] \qquad (2.10)
\end{aligned}$$

where, $\sqrt{\omega_m^2 - \omega_b^2} = \omega_m(\sqrt{1 - \zeta_m^2}) = \omega_{dm}$,where $\omega_{dm}$is the damped natural frequency of mTh mode.

Let,

$$\begin{aligned}
U_m^p(t) &= U \sin(m\Omega t - \theta) \\
&= U(\sin m\Omega t \cos\theta - \cos m\Omega t \sin\theta) \\
&= U \cos\theta \sin m\Omega t - U \sin\theta \cos m\Omega t
\end{aligned}$$

Also, Let,

$$\begin{aligned}
U\cos\theta &= U_1 \\
U\sin\theta &= U_2 \\
\theta &= \tan^{-1}\frac{U_2}{U1}
\end{aligned}$$

So,

$$\begin{aligned}
U_m^p(t) &= U_1 \sin m\Omega t - U_2 \cos m\Omega t \\
\therefore \dot{U}_m^p(t) &= m\Omega(U_1 \cos m\Omega t + U_2 \sin m\Omega t) \\
\therefore \ddot{U}_m^p &= (m\Omega)^2\left[-U_1 \sin m\Omega t + U_2 \cos m\Omega t\right]
\end{aligned}$$

From Eq.(2.8),

$(m\Omega)^2\left[-U_1 \sin m\Omega t + U_2 \cos m\Omega t\right] + 2\omega_b\left[m\Omega(U_1 \cos m\Omega t + U_2 \sin m\Omega t)\right] + \omega_m^2(U_1 \sin m\Omega t - U_2 \cos m\Omega t) = \frac{Pl}{2\mu}\sin(m\Omega t)$

$\Rightarrow \left[-U_1(m\Omega)^2 + 2\omega_b m\Omega U_2 + \omega_m^2 U_1 - \frac{Pl}{2\mu}\right]\sin m\Omega t + \left[(m\Omega)^2 U_2 + 2\omega_b m\Omega U_1 - \omega_m^2 U_2\right]\cos m\Omega t = 0$

$$(m\Omega)^2\left[-U_1\sin m\Omega t + U_2\cos m\Omega t\right] + 2\omega_b\left[m\Omega(U_1\cos m\Omega t + U_2\sin m\Omega t)\right] + \omega_m^2(U_1\sin m\Omega t - U_2\cos m\Omega t) = \frac{Pl}{2\mu}\sin(m\Omega t)$$

$$\left[-U_1(m\Omega)^2 + 2\omega_b m\Omega U_2 + \omega_m^2 U_1 - \frac{Pl}{2\mu}\right]\sin m\Omega t + \left[(m\Omega)^2 U_2 + 2\omega_b m\Omega U_1 - \omega_m^2 U_2\right]\cos m\Omega t = 0 \tag{2.11}$$

Since Eq.(2.11) is true for all t,equating the sinand cos terms from both the sides gives,

$$\left[-(m\Omega)^2 + \omega_m^2\right]U_1 + 2\omega_b m\Omega U_2 = \frac{Pl}{2\mu}$$

$$2\omega_b m\Omega U_1 + \left[(m\Omega)^2 - \omega_m^2\right]U_2 = 0$$

or in matrix form,

$$\begin{bmatrix} \omega_m^2 - (m\Omega)^2 & 2\omega_b m\Omega \\ 2\omega_b m\Omega & (m\Omega)^2 - \omega_m^2 \end{bmatrix}\begin{Bmatrix} U_1 \\ U_2 \end{Bmatrix} = \begin{Bmatrix} \frac{Pl}{2\mu} \\ 0 \end{Bmatrix} \tag{2.12}$$

Let,

$$M = \begin{bmatrix} \omega_m^2 - (m\Omega)^2 & 2\omega_b m\Omega \\ 2\omega_b m\Omega & (m\Omega)^2 - \omega_m^2 \end{bmatrix}$$

From Eq.(2.12)

$$\begin{Bmatrix} U_1 \\ U_2 \end{Bmatrix} = M^{-1}\begin{Bmatrix} \frac{Pl}{2\mu} \\ 0 \end{Bmatrix} = \frac{1}{-\left[\omega_m^2 - (m\Omega)^2\right]^2 - (2\omega_b m\Omega)^2}\begin{Bmatrix} \frac{Pl}{2\mu}[(m\Omega)^2 - \omega_m^2] \\ \frac{Pl}{2\mu}[-2\omega_b m\Omega] \end{Bmatrix} \tag{2.13}$$

Thus the particular solution is

$$V_m^p(t) = U_1\sin m\Omega t - U_2\cos m\Omega t$$

where, $U_1$and $U_2$are given by Eq.(2.13)
The total Solution is

$$U_m(t) = U_m^c(t) + U_m^p(t)$$

$$U_m(t) = e^{-\omega_b t}[A_1\cos\omega_{dm}t + A_2\sin\omega_{dm}t] + \frac{Pl}{2\mu}\frac{1}{-\left[\omega_m^2 - (m\Omega)^2\right]^2 - (2\omega_b m\Omega)^2}\left[\left\{(m\Omega)^2 - \omega_m^2\right\}\sin m\Omega t + 2\omega_b m\Omega\cos m\Omega t\right] \tag{2.14}$$

At $t = 0$, $U_m(0) = 0$.

$$\therefore A_1 = \frac{Pl}{2\mu} \frac{2\omega_b m\Omega}{\left[\omega_m^2 - (m\Omega)^2\right]^2 + (2\omega_b m\Omega)^2}$$

At $t = 0, \dot{U}_m(0) = 0$

$$\therefore A_2 = \frac{Pl}{2\mu} \frac{m\Omega}{\omega_{dm}} \frac{2\omega_b^2 + (m\Omega)^2 - \omega_m^2}{\left[\omega_m^2 - (m\Omega)^2\right]^2 + (2\omega_b m\Omega)^2}$$

Governing Equation,

$$\ddot{U}_m(t) + 2\omega_b \dot{U}_m(t) + \omega_m^2 U_m(t) = 0 \tag{2.15}$$

Initial conditions for equation of $t \geq T$ is obtained from the solution of the equation of $t \leq T$ evaluated at the $t = T$.

So,the initial conditions(From Eq.(2.14) evaluating at $t = T$) for Eq.(2.15) are,

$$U_m(T) = e^{-\omega_b T}[A_1 \cos\omega_{dm} T + A_2 \sin\omega_{dm} T] + \frac{Pl}{2\mu} \frac{1}{-\left[\omega_m^2 - (m\Omega)^2\right]^2 - (2\omega_b m\Omega)^2} \left[\left\{(m\Omega)^2 - \omega_m^2\right\} \sin m\Omega T + 2\omega_b m\Omega \cos m\Omega T\right]$$

$$\dot{U}_m(T) = -\omega_b e^{-\omega_b T}(A_1 \cos\omega_{dm} T + A_2 \sin\omega_{dm} T) + \omega_{dm} e^{-\omega_b T}(-A_1 \sin\omega_{dm} T + A_2 \cos\omega_{dm} T) + \frac{Pl}{2\mu} \frac{1}{-\left[\omega_m^2 - (m\Omega)^2\right]^2 - (2\omega_b m\Omega)^2} * \left[\left\{(m\Omega)^2 - \omega_m^2\right\} \sin m\Omega t + 2\omega_b m\Omega \cos m\Omega t\right]$$

Let,

$$U_m(T) = U_{mT}$$

$$\dot{U}_m(T) = \dot{U}_{mT}$$

Solution of the Eq.(2.15) is similar to that of Eq.(2.10).

$U_m(t) = e^{-\omega_b(t-T)}[A_{11} \cos\omega_{dm}(t-T) + A_{22} \sin\omega_{dm}(t-T)]$

$\dot{U}_m(t) = -\omega_b e^{-\omega_b(t-T)}[A_{11} \cos\omega_{dm}(t-T) + A_{22} \sin\omega_{dm}(t-T)] + \omega_{dm} e^{-\omega_b(t-T)}[-A_{11} \sin\omega_{dm}(t-T) + A_{22} \cos\omega_{dm}(t-T)]$

$$U_m(t) = e^{-\omega_b(t-T)}[A_{11} \cos\omega_{dm}(t-T) + A_{22} \sin\omega_{dm}(t-T)] \tag{2.16}$$

$$\begin{aligned} \dot{U}_m(t) &= -\omega_b e^{-\omega_b(t-T)}[A_{11} \cos\omega_{dm}(t-T) + A_{22} \sin\omega_{dm}(t-T)] \\ &\quad + \omega_{dm} e^{-\omega_b(t-T)}[-A_{11} \sin\omega_{dm}(t-T) + A_{22} \cos\omega_{dm}(t-T)] \end{aligned} \tag{2.17}$$

At $t = T$, from Eq.(2.16) and (2.17),

$$U_{mT} = A_{11}$$
$$\dot{U}_{mT} = -\omega_b A_{11} + A_{22}\omega_{dm}$$

Therefore,

$$\begin{aligned} A_{11} &= U_{mT} \\ A_{22} &= \frac{1}{\omega_{dm}}(\omega_b A_{11} + \dot{U}_{mT}) \end{aligned} \tag{2.18}$$

So, the solution for $t \geq T$ is given by Eq.(2.16) together with Eq.(2.18)

Chapter 3

Piezoelectric Energy Harvester

The term "piezo" is derived from the Greek word for pressure. In 1880 Jacques and Pierre Curie discovered that an electric potential could be generated by applying pressure to quartz crystals; they named this phenomenon the "piezo effect". Later they ascertained that when exposed to an electric potential, piezoelectric materials change shape. This they named the "inverse piezo effect". The first commercial applications of the inverse piezo effect were for sonar systems that were used in World War I. A break through was made in the 1940's when scientists discovered that barium titanate could be bestowed with piezoelectric properties by exposing it to an electric field[25]

The following few sections are adopted from [26].

3.1 Piezoelectric Effect

Figure 3.1(a)shows a simple molecular model; it explains the generating of an electric charge as the result of a force exerted on the material. Before subjecting the material to some external stress, the gravity centres of the negative and positive charges of each molecule coincide. Therefore, the external effects of the negative and positive charges are reciprocally cancelled. As a result, an electrically neutral molecule appears. When exerting some pressure on the material, its internal reticular structure can be deformed, causing the separation of the positive and negative gravity centres of the molecules and generating little dipoles (Figure 3.1(b)). The facing poles inside the material are mutually cancelled and a distribution of a linked charge appears in the material's surfaces (Figure 3.1(c)). That is to say, the material is polarized. This polarization generates an electric field and can be used to transform the mechanical energy used in the material's deformation into electrical energy.

Figure 3.2(a) shows the piezoelectric material on which a pressure is applied. Two metal plates used as electrodes are deposited on the surfaces where the linked charges of opposite sign appear. Let us suppose that those electrodes are externally short circuited through a wire to which a galvanometer has been connected. When exerting some pressure on the piezoelectric material, a linked charge density appears on the surfaces of the crystal in contact with the electrodes. This polarization generates an electric field which causes the flow of the free charges existing in the conductor. Depending on their sign, the free charges will move towards the ends where the linked charge generated by the crystal's polarization is of opposite sign. This flow of free charges will remain until the free charge neutralizes the polarization effect (Figure3.2(a)). When the pressure on the crystal stops, the polarization will disappear, and the flow of free charges will be reversed, coming back to the initial standstill condition (Figure 3.2(b)). This process would be displayed in the galvanometer, which would have marked two opposite sign current peaks. If a resistance is connected instead of a

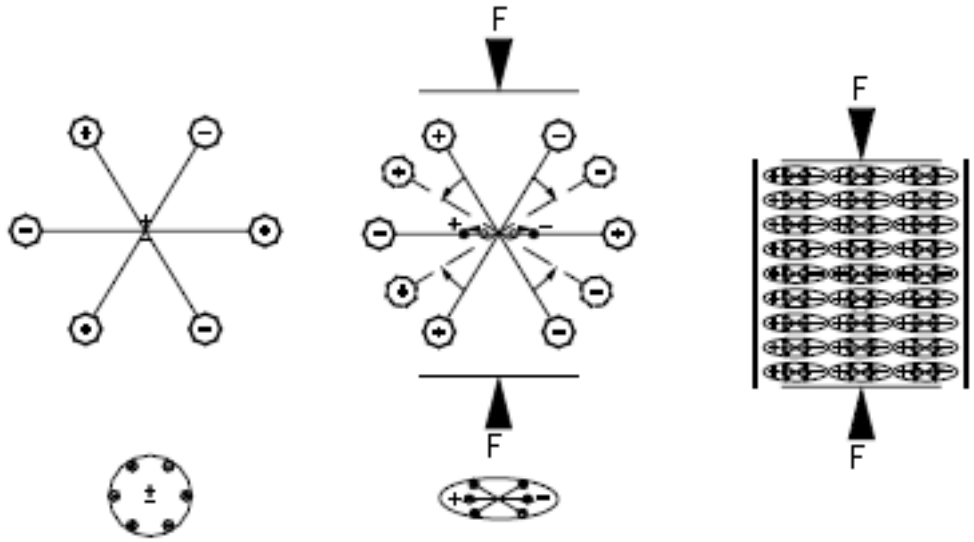

Figure 3.1: Simple molecular model for explaining the piezoelectric effect: a unperturbed molecule; b molecule subjected to an external force, and c polarizing effect on the material surfaces[26]

short-circuiting, and a variable pressure is applied, a current would flow through the resistance, and the mechanical energy would be transformed into electrical energy.

The Curie brothers verified, the year after their discovery, the existence of the reverse process, predicted by Lippmann (1881) [26]. That is, if one arbitrarily names direct piezoelectric effect, to the generation of an electric charge, and hence of an electric field, in certain materials and under certain laws due to a stress, there would also exist a reverse piezoelectric effect by which the application of an electric field, under similar circumstances, would cause deformation in those materials. In this sense, a mechanical deformation would be produced in a piezoelectric material when a voltage is applied between the electrodes of the piezoelectric material, as shown in Figure 3.2. This strain could be used, for example, to displace a coupled mechanical load, transforming the electrical energy into mechanical energy.

3.2 Mathematical Formulation of Piezoelectric Effect:A First Approach

In a first approach, the experiments performed by the Curie brothers demonstrated that the surface density of the generated linked charge was proportional to the pressure exerted, and would disappear with it. This relationship can be formulated in a simple way as follows:

$$P_p = dT$$

where P_p is the piezoelectric polarization vector, whose magnitude is equal to the linked charge surface density by piezoelectric effect in the considered surface, d is the piezoelectric strain coefficient and T is the stress to which the piezoelectric material is subjected. The Curie brothers verified the reverse piezoelectric effect and demonstrated that the ratio between the strain produced and the magnitude of the applied electric field in the reverse effect, was equal to the ratio between the produced polarization and the magnitude of the applied stress in the direct effect. Consistently, the reverse piezoelectric effect can be formulated in a simple way, as a first approach, as follows:

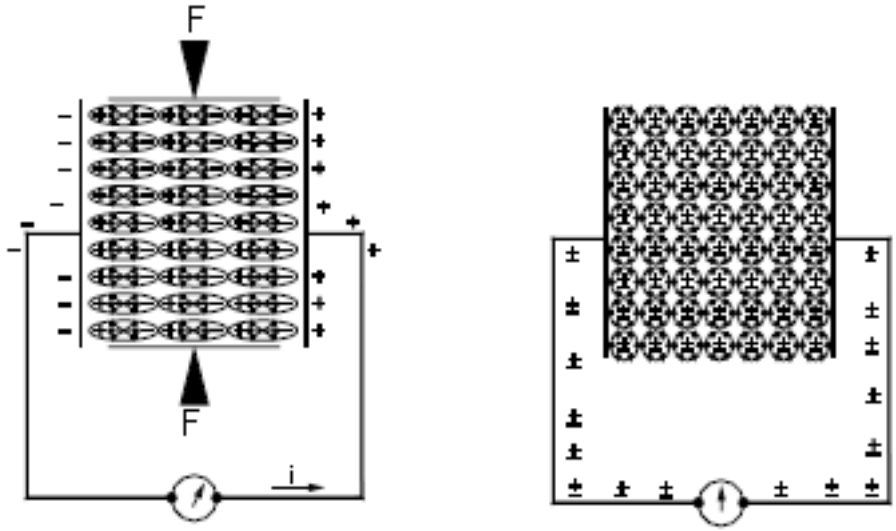

a b

Figure 3.2: Piezoelectric phenomenon: a neutralizing current flowing through the short-circuiting established on a piezoelectric material subjected to an external force; b absence of current through the short-circuited material in an unperturbed state[26]

$$S_p = dE$$

where S_p is the strain produced by the piezoelectric effect and E is the magnitude of the applied electric field. The direct and reverse piezoelectric effects can be alternatively formulated, considering the elastic properties of the material, as follows:

$$P_p = dT = dcS = eS \tag{3.1}$$

$$T_p = cS_p = cdE = eE$$

where c is the elastic constant, which relates the stress generated by the application of a strain ($T = cS$), s is the compliance coefficient which relates the deformation produced by the application of a stress ($S = sT$), and$e$ is the piezoelectric stress constant. (Note that the polarizations, stresses, and strains caused by the piezoelectric effect have been specified with the p subscript, while those externally applied do not have subscript.)

3.3 Piezoelectric Contribution To Elastic Constants

The piezoelectric phenomenon causes an increase of the material's stiffness. To understand this effect, let us suppose that the piezoelectric material is subjected to a strain S. This strain will have two effects. On the one hand, it will generate an elastic stress T_e which will be proportional to the mechanical strain $T_e = cS$; on the other hand, it will generate a piezoelectric polarization $P_p = eS$ according to Eq.(4.1). This polarization will create an internal electric field in the material E_p given by :

$$E_p = \frac{P_p}{\varepsilon} = \frac{eS}{\varepsilon}$$

where ε is the dielectric constant of the material. This electric field, of piezoelectric origin, produces a force against the deformation of the material's electric structure, creating a stress $T_p = eE_p$. This stress, as well as that of elastic origin, is against the material's deformation. Consistently, the stress generated as a consequence of the strain S will be:

$$T = T_e + T_p = cS + \frac{e^2}{\varepsilon}S = \left(c + \frac{e^2}{\varepsilon}\right)S = \bar{c}S$$

Therefore, the constant $\bar{c}$ is the piezoelectrically stiffened constant, which includes the increase in the value of the elastic constant due to the piezoelectric effect.

3.4 Piezoelectric Contribution To Dielectric Constants

When an external electric field E is applied between two electrodes where a material of dielectric constant ε exists, an electric displacement is created towards those electrodes, generating a surface charge density$\sigma = \sigma_o + \sigma_d$which magnitude is $D = \varepsilon E$. If that material is piezoelectric, the electric field E produces a strain given by: $S_p = dE$. This strain of piezoelectric origin increases the surface charge density due to the material's polarization in an amount given by: $P_p = eS_p = edE$ (Figure 3.3). Because the electric field is maintained constant, the piezoelectric polarization increases the electric displacement of free charges towards the electrodes in the same magnitude ($\sigma_p = P_p$). Therefore, the total electrical displacement is:

$$D = \varepsilon E + P_p = \varepsilon E + edE = \bar{\varepsilon}E$$

where $\bar{\varepsilon}$ is the effective dielectric constant which includes the piezoelectric contribution.

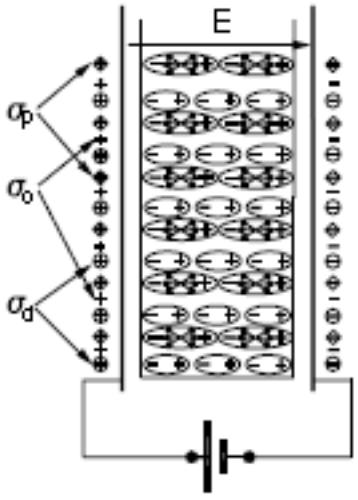

Figure 3.3: Schematic diagram that explains different electrical displacements associated with a piezoelectric and dielectric material[26]

3.5 The Electric Displacement and The Internal Stress

As shown in the previous paragraph, the electric displacement produced when an electric field E is applied to a piezoelectric and dielectric material is

$$D = \varepsilon E + P_p = \varepsilon E + eS_p$$

Under the same circumstances we want to obtain the internal stress in the material. The reasoning is the following: the application of an electric field on a piezoelectric material causes a deformation in the material's structure given by: $S_p = dE$. This strain produces an elastic stress whose magnitude is $T_e = cS_p$. On the other hand, the electric field E exerts a force on the material's internal structure generating a stress given by: $T_p = eE$. This stress is, definitely, the one that produces the strain and is of opposite sign to the elastic stress which tends to recover the original structure. Therefore, the internal stress that the material experiences will be the resultant of both. That is:

$$T = cS_p - eE$$

Eventually, both stresses will be equal leaving the material strained and static. If a variable field is applied, as it is the common practice, the strain will vary as well, producing a dynamic displacement of the material's particles. This electromechanical phenomenon generates a perturbation in the medium in contact with the piezoelectric material.

3.6 Piezoelectric Model[27]

Up to now, to deal with piezoelectric constitutive equations, no attention was paid to the poling direction. But Piezoelectricity of a material is affected by the Polarising direction. So, the more accurate and customed(IEEE standard on Piezoelectricity) way of representing piezoelectric constitutive equations are given by :

$$\text{Direct Piezoelectric Effect:} D = e.S + \varepsilon^S.E$$

$$\text{Converse Piezoelectric Effect:} T = c^E.S - e^t.E$$

or in matrix form,

$$\begin{Bmatrix} D \\ T \end{Bmatrix} = \begin{bmatrix} e & \varepsilon^S \\ c^E & -e^t \end{bmatrix} \begin{Bmatrix} S \\ E \end{Bmatrix} \tag{3.2}$$

Let us consider 1-D piezoelectric model of the Figure 3.4. The piezoelectric element is excited by a base input displacement, y_b. The piezoelectric element has a mass M_p and is connected to a power-harvesting circuit, modeled simply as a resistor. A proof mass, M, is also considered. Electrode thicknesses are taken to zero (i.e., ignored) in the analysis. Note that the entire structure is electromechanically coupled in this example, whereas in energy harvesters such as uni-morph/bi-morph configurations, a portion of the structure will be inactive.

For this model, the equation (3.2) can be simplified to,

$$D_3 = e_{33}S_3 + \varepsilon^S_{33}E_3 \tag{3.3}$$

$$T_{33} = c^E_{33}S - e^t_{33}E_{33} \tag{3.4}$$

The D, E, S, and T matrices are defined as developed electric displacement, applied electric field, applied strain, and developed stress, respectively.e is also referred to as the piezoelectrically induced stress tensor as it relates the stress to electric field. c^E is the stiffness matrix. The superscripts E

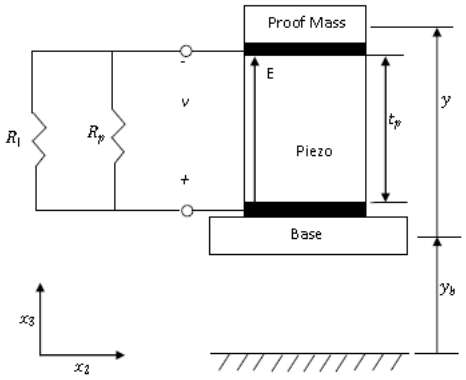

Figure 3.4: 1D Piezoelectric energy harvester model

and S indicate a parameter at constant (typically zero) electric field and strain respectively, while superscript t indicates the transpose of the matrix.

From a force equilibrium analysis, the governing equations can be found in terms of the constitutive relations (Eqs.(3.3) and (3.4)) and device parameters, defined in Figure (3.4). The piezoelectric element is poled in the x_3 direction. The strain is related to the device parameters through $S_3 = \frac{y}{t_p}$ and the electric field is defined as $E_3 = -\frac{v}{t_p}$, y is the relative displacement in the figure. The approximate total mass[1] of the system is $m_t = M + \frac{1}{3}M_p$and $m = \frac{m_t}{A_p}$is the mass per cross sectional area. $A_p$is the cross sectional area of the electrodes(or the piezoelectric element).The stress is the force per area, or $T_3 = -\frac{m_t(\ddot{y}+\ddot{y}_b)}{A_p} = -m(\ddot{y} + \ddot{y}_b)$. y_b is the base acceleration and q is the charge developed on the electrodes. The overhead dot indicates the time derivative of the variable. The electric displacement, D_3, is the charge on the electrodes per unit area. These all give,

$$m\ddot{y} + c_{33}^E \frac{y}{t_p} + e_{33}\frac{v}{t_p} = -m_e\ddot{y}_b \tag{3.5}$$

$$D_3 = e_{33}\frac{x}{t_p} - \varepsilon_{33}^S \frac{v}{t_p} = \frac{q}{A_p} \tag{3.6}$$

Both equations are multiplied by $A_p$and a convenient electromechanical coupling term $\theta = -\frac{e_{33}A_p}{t_p}$, is defined. Furthermore, $k = \frac{c_{33}^E A_p}{t_p}$is the effective stiffness. The capacitance is defined in terms of the constrained permittivity: $C_p = \frac{\varepsilon_{33}^S A_p}{t_p}$. The overhead dot indicates the time derivative. The second governing equation (sensing equation), Eq.(3.6), can be written in terms of the current, $i = \frac{dq}{dt}$, by taking the time derivative. For the purely resistive electrical load (as has been assumed), the current can be related to the voltage developed through $v = iR_p$. The equivalent resistance, R_p, is the parallel resistance of the load and the leakage resistances, R_l and R_p respectively. In general, the leakage resistance is much higher than the load resistance [27], so that $R_p \approx R_l$. With these definitions and substitutions, Eqs.(3.7) and (3.8) are obtained from Eqs. (3.5) and (3.6).

$$m\ddot{y} + ky - \theta v = -m\ddot{y}_b \tag{3.7}$$

$$\theta\dot{y} + C_p\dot{v} + \frac{1}{R_l}v = 0 \tag{3.8}$$

[1] 1For longitudinal vibrations of a rod, the resonance frequency is often estimated by lumping one third of the mass of the rod at the tip. Together with the proof mass, this defines an approximate effective mass for the system.

Note that Eq.(3.7), without the θv coupling term, is the familiar dynamic equation of motion for a 1 degree-of-freedom spring-mass system. If viscous damping, c_d (proportional to the velocity $\dot{y}$) is added to the system, the total model is represented by the equations,

$$m\ddot{y} + c_d\dot{y} + ky - \theta v = -m\ddot{y}_b \tag{3.9}$$

$$\theta\dot{y} + C_p\dot{v} + \frac{1}{R_l}v = 0 \tag{3.10}$$

The initial conditions are assumed as follows:

At $t = 0$, $y = 0$

$y_b = 0$

$\dot{y} = 0$

$\dot{y}_b = 0$

3.6.1 Frequency domain representation

Taking Laplace transform[28] of Eq.(3.9) and applying initial conditions,

$$m\left[s^2Y(s) - sy(0) - \dot{y}(0)\right] + c\left[sY(s) - y(0)\right] + kY(s) - \theta V(s) = -m\left[s^2Y_b(s) - sy_b(0) - \dot{y}_b(0)\right]$$
$$\left[ms^2 + cs + k\right]Y(s) - \theta V(s) = -ms^2Y_b(s)$$

Putting $s = j\omega$,

$$\left[m(j\omega)^2 + c(j\omega) + k\right]Y(\omega) - \theta V(\omega) = m(j\omega)^2Y_b(\omega)$$
$$\left[-m\omega^2 + jc\omega + k\right]Y(\omega) - \theta V(\omega) = m\omega^2Y_b(\omega)$$
$$\left[-\omega^2 + j\frac{c}{m}\omega + \frac{k}{m}\right]Y(\omega) - \frac{\theta}{m}V(\omega) = \omega^2Y_b(\omega)$$
$$(-\omega^2 + 2j\omega\zeta_h\omega_h + \omega_h^2)Y(\omega) - \frac{\theta}{m}V(\omega) = \omega^2Y_b(\omega)$$

where,natural frequency of the energy harvester, $\omega_h = \sqrt{\frac{k}{m}}$and the harvester damping,$\zeta_h = \frac{c}{2m\omega_h}$

Dividing by ω_h^2,

$$(-\frac{\omega^2}{\omega_h^2} + 2j\frac{\omega}{\omega_h}\zeta_h + 1)Y(\omega) - \frac{\theta}{m\omega_h^2}V(\omega) = \frac{\omega^2}{\omega_h^2}Y_b(\omega)$$

Let,$\Omega_h = \frac{\omega}{\omega_h}$

$$\left[\left(1 - \Omega_h^2\right) + 2j\zeta_h\Omega_h\right]Y(\omega) - \frac{\theta}{k}V(\omega) = \Omega_h^2Y_b(\omega)$$

Taking Laplace transform of Eq.(3.9) and (3.10)

$$s\left[sY(s)-y(0)\right]+C_p\left[sV(s)-v(0)\right]+\frac{1}{R_l}V(s)=0$$
$$\left[\theta sY(s)+(C_ps+\frac{1}{R_l})V(s)\right]=0$$

Putting $s=j\omega$, and dividing by C_p,

$$j\omega\frac{\theta}{C_p}Y(\omega)+\left(j\omega+\frac{1}{C_pR_l}\right)V(\omega)=0$$

Again Dividing by ω_h,

$$j\frac{\omega}{\omega_h}\frac{\theta}{C_p}Y(\omega)+\left(j\frac{\omega}{\omega_h}+\frac{1}{C_pR_l\omega_h}\right)V(\omega)=0$$

Let, $\alpha=\omega_hC_pR_l$

$$j\Omega_h\frac{\theta}{C_p}Y(\omega)+\left(j\Omega_h+\frac{1}{\alpha}\right)V(\omega)=0$$
$$j\Omega_h\frac{\alpha\theta}{C_p}Y(\omega)+\left(j\Omega_h\alpha+1\right)V(\omega)=0$$

In Matrix Form,

$$\begin{bmatrix}\left(1-\Omega_h^2\right)+2j\zeta_h\Omega & -\frac{\theta}{k}\\ j\Omega_h\frac{\alpha\theta}{C_p} & (j\Omega_h\alpha+1)\end{bmatrix}\begin{Bmatrix}Y(\omega)\\V(\omega)\end{Bmatrix}=\begin{Bmatrix}\Omega_h^2Y_b(\omega)\\0\end{Bmatrix}\tag{3.11}$$

Let,

$$M=\begin{bmatrix}\left(1-\Omega_h^2\right)+2j\zeta_h\Omega_h & -\frac{\theta}{k}\\ j\Omega_h\frac{\alpha\theta}{C_p} & (j\Omega_h\alpha+1)\end{bmatrix}$$
$$\begin{aligned}\det M&=\left[\left(1-\Omega_h^2\right)+2j\zeta_h\Omega_h\right](j\Omega_h\alpha+1)-\left(-\frac{\theta}{k}\right)j\Omega_h\frac{\alpha\theta}{C_p}\\&=j\Omega_h\alpha-j\Omega_h^3\alpha+1-\Omega_h^2+(-2\zeta_h\Omega_h^2\alpha)+2j\zeta_h\Omega_h+\frac{\alpha\theta^2}{kC_p}\\&=(j\Omega_h)^3\alpha+(2\zeta\alpha+1)(j\Omega_h)^2+(\alpha+\kappa^2\alpha+2\zeta_h)(j\Omega_h)+1\\&=\Delta_l(j\omega)\end{aligned}$$

where,$\frac{\theta^2}{kC_p}=\kappa^2$ and $\Delta_l(j\omega)=(j\Omega_h)^3\alpha+(2\zeta_h\alpha+1)(j\Omega_h)^2+(\alpha+\kappa^2\alpha+2\zeta_h)(j\Omega_h)+1$
So, from Eq.(3.11),

$$
\begin{aligned}
M^{-1}M \begin{Bmatrix} Y(\omega) \\ V(\omega) \end{Bmatrix} &= M^{-1} \begin{Bmatrix} \Omega^2 Y_b(\omega) \\ 0 \end{Bmatrix} \\
\begin{Bmatrix} Y(\omega) \\ V(\omega) \end{Bmatrix} &= \frac{1}{\Delta_l} \begin{bmatrix} (j\Omega\alpha + 1) & -\dfrac{\theta}{k} \\ j\Omega\dfrac{\alpha\theta}{C_p} & \left(1-\Omega^2\right) + 2j\zeta_h\Omega \end{bmatrix} \begin{Bmatrix} \Omega^2 Y_b(\omega) \\ 0 \end{Bmatrix} \\
&= \begin{Bmatrix} (j\Omega\alpha + 1)\,\Omega^2 Y_b(\omega)/\Delta_l \\ j\Omega\dfrac{\alpha\theta}{C_p}\Omega^2 Y_b(\omega)/\Delta_l \end{Bmatrix}
\end{aligned} \tag{3.12}
$$

Eq.(3.12)gives the frequency domain representation of the displacement y of Eq.(3.9) and voltage$v$ of Eq.(3.10) through $Y(\omega)$and $V(\omega)$respectively.So, in other way, Eq.(3.12)is the frequency domain representation of the 1D energy harvester of Figure 3.4

Chapter 4

Mathematical Modelling and Results

The previous two chapters were devoted to develop the theory of the bridge dynamics under a moving constant load and 1D modelling approach of a simple Piezoelectric energy harvester, respectively. Based on these a novel idea is presented in this chapter combining these two. The feasibility of the concept of using bridge vibration as an input to the Piezoelectric energy harvester is studied in terms of micro scale power production with the help of an adopted theoretical example.

4.1 Mathematical Model of Energy Harvester for Bridge

In Chapter (2), the bridge dynamics under a constant moving load was discussed. The frequency domain solution of the bridge deflection is given by Eq. (2.7) as,

$$\begin{aligned} U(x,\omega) \quad &= \sum_{n=1}^{\infty} \quad \frac{1}{(-\omega_n^2 + 4j\omega\zeta_n\omega_n + \omega_n^2)} \frac{1}{\sqrt{2\pi}} \frac{Pl}{2\mu} \frac{1}{2j} * \\ &* \quad \left(\frac{e^{j(n\Omega-\omega)T}}{j(n\Omega-\omega)} + \frac{e^{j(n\Omega-\omega)T}}{j(n\Omega+\omega)} - \frac{1}{j(n\Omega-\omega)} + \frac{1}{j(n\Omega+\omega)} \right) \sin\left(\frac{n\pi x}{l}\right) \end{aligned} \tag{4.1}$$

where the symbols having the same meaning as in Chapter 2.

From Chapter 3, the 1D Piezoelectric energy harvester model's deflection as input and generated voltage as output is given by Eq.(3.12) as,

$$\left\{ \begin{array}{c} Y(\omega) \\ V(\omega) \end{array} \right\} = \left\{ \begin{array}{c} (j\Omega\alpha + 1)\,\Omega^2 Y_b(\omega)/\Delta_l \\ j\Omega\dfrac{\alpha\theta}{C_p}\Omega^2 Y_b(\omega)/\Delta_l \end{array} \right\} \tag{4.2}$$

where, $\dfrac{\theta^2}{kC_p} = \kappa^2$, $\Delta_l(j\omega) = (j\Omega)^3\alpha + (2\zeta\alpha + 1)(j\Omega)^2 + (\alpha + \kappa^2\alpha + 2\zeta)(j\Omega) + 1$ and the symbols having the same meaning as previous.

The second of Eq.(3.2) gives the generated voltage $V(\omega)$, in terms of the base deflection $Y_b(\omega)$ of the harvester. This base deflection is obtained from the structure on which the harvester is mounted, for the case under consideration it is the bridge. Hence, the bridge deflection $U(x,\omega)$ given by Eq.(4.1) is nothing but the profile of the harvester deflection $Y_b(\omega)$ under the moving load condition as the harvester is mounted on the bridge.[1]

Power ooutput is given by,

$$Power = \frac{V^2}{R_l} \tag{4.3}$$

[1]It is assumed that at a specific location,x of the bridge the deflection of the bridge and the harvester are same i.e. $U(x,\omega) \approx Y(\omega)$

where V is the voltage from the Eq.(4.2) and $R_l$is the load resistance set to the circuit.

4.2 Example.

The best way to get the insight into the developed physical system is to assign numerical values to constants and then change the parameters to identify their relative interactions. With this end in mind, for the bridge model the following data are adopted[30][2]The bridge is considered to be under a moving load of $1000N$.

Table 4.1: Bridge parameters[29]

Bridge parameter	Value
Crossectional Area, A	$2m^2$
Mass per unit length,μ	$4800kg/m$
Elastic modulus,E	$27.5GN/m^2$
Moment of inertia,I	$0.12m^4$

Similarly, a Piezoelectric energy harvester, as shown in the Figure 4.1, of PVDF(Polyvinylidine fluoride) material is adopted[30].The stave is laminated in a bi morph design around a 1mm plastic substrate. Sheets of 28 micron PVDF were inked with a stretched hexagon electrode pattern and laminated in two 8-layer stacks on each side of the substrate as in Figure 4.1.

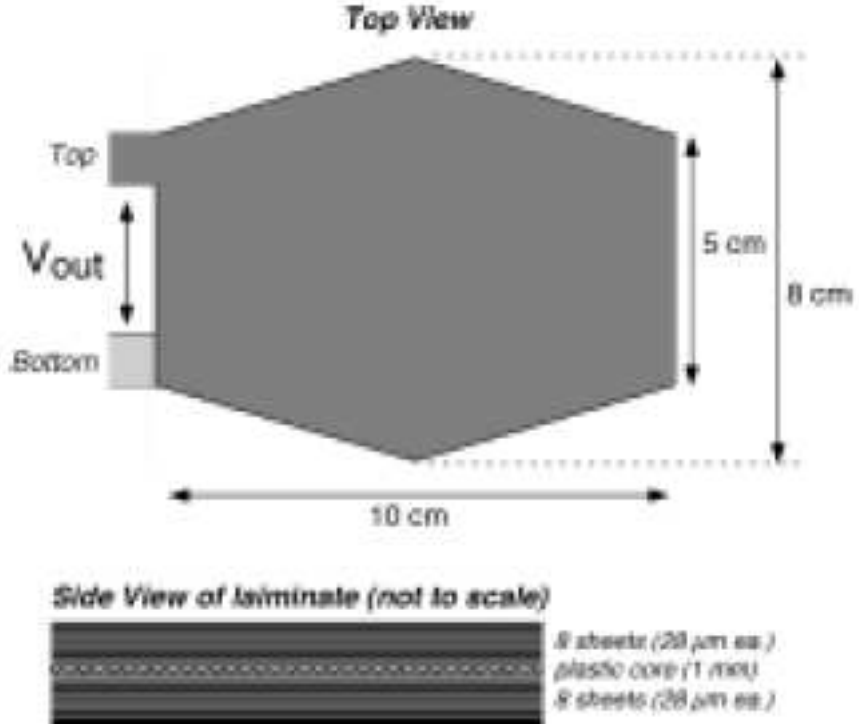

Figure 4.1: PVDF Stave(Top and Side View)[30]

The properties of this stave are as follow:

[2]Due to inaccessibility of practical verification opportunities, the bridge and the harvester data are adopted instead of preparing a test specimen

Table 4.2: PVDF Stave Properties[30]

Property	Symbol	Value	Units
Young's Modulus	E	2.4	$10^9 N/m^2$
Piezo Stress Constant	e_{31}	75	$10^{-3} C/m^2$
Total Area(For 16 Sheet)	A	0.104	m^2
Thickness	t	28	$10^{-6} m$
Capacitance	C_p	330	$10^{-9} F$
Damping ratio	ξ	0.0385	
Density	ρ	1.78	$10^3 Kg/m^3$
Frequency	ω_h	2	Hz

Based on table(4.2), the following parameters are calculated,

$$\begin{aligned} \text{Mass}, M_h &= \rho A t \\ &= 1.78 * 0.104 * 28 * 10^{-6} \\ &= 5.18336 * 10^{-6} kg \end{aligned}$$

$$\begin{aligned} \text{Spring Constant}, K_h &= \omega_h^2 * M \\ &= (2 * 6.28)^2 * 5.18336 * 10^{-6} \\ &= 1.489 * 10^{-4} N/m \end{aligned}$$

$$\begin{aligned} \text{Electromechanical Coupling}, \theta &= -\frac{e_{31} A_p}{t_p} \\ &= -\frac{0.075 * 0.104}{28 * 10^{-6}} \\ &= -278.57 C/m \end{aligned}$$

Load resistance of the harvester circuit was set at $200K\Omega$
Therefore,

$$\begin{aligned} \text{Dimensionless time constant}, \alpha &= \omega_h C_p R_l \\ &= 2 * 6.28 * 330 * 10^{-9} * 200 * 10^3 \\ &= 0.173448 \end{aligned}$$

4.3 Results

Based on this numerical model, the output power is examined changing the harvester position, vehicle velocity, bridge length and corresponding bridge damping. A summarized result is presented in the table(4.3),(4.4) and (4.5). It is followed by graphs of maximum power output for different bridge lengths for each harvester position.

Table 4.3: Piezoelectric energy harvester placed at $\frac{1}{4}$Th of the bridge length

Bridge length,$l(m)$	Velocity,c (mi/hr)	Maximum Power,$\frac{V^2}{R}(10^{-6}W)$	Maximum Power$(10^{-6}W)$	Velocity,$c(mi/hr)$
25	20	0.1223	1.013	40
	40	1.013		
	60	0.4933		
	80	0.143		
	100	0.3136		
50	20	52.07	52.07	20
	40	9.795		
	60	14.4		
	80	4.956		
	100	2.492		
75	20	52.1	148.5	40
	40	148.5		
	60	35.01		
	80	15.84		
	100	13.19		
100	20	592.5	592.3	20
	40	282.3		
	60	87.45		
	80	55.64		
	100	53.59		

Table 4.4: Piezoelectric energy harvester placed at $\frac{1}{2}$Th of the bridge length

Bridge length,lm	Velocity,c (mi/hr)	Maximum Power,$\frac{V^2}{R}(10^{-6}W)$	Maximum Power$(10^{-6}W)$	Velocity$c(mi/hr)$
25	20	0.0243	2.032	40
	40	2.032		
	60	0.9897		
	80	0.3909		
	100	0.1295		
50	20	124.5	124.5	20
	40	19.45		
	60	4.784		
	80	6.03		
	100	3.974		
75	20	104.6	104.6	20
	40	9.875		
	60	73.74		
	80	23		
	100	26.9		
100	20	9.72	141.13	40
	40	141.3		
	60	47.16		
	80	114.1		
	100	50.34		

Table 4.5: Piezoelectric energy harvester placed at $\frac{3}{4}$Th of the bridge length

Bridge length,lm	Velocity,c (mi/hr)	Maximum Power,$\frac{V^2}{R}(10^{-6}W)$	Maximum Power $(10^{-6}W)$	Velocity,$c(mi/hr)$
25	20	0.1199	1.019	40
	40	1.019		
	60	0.4956		
	80	0.15		
	100	0.3255		
50	20	52.44	52.44	20
	40	9.954		
	60	15.09		
	80	4.904		
	100	2.729		
75	20	52.48	154.6	40
	40	154.6		
	60	37.84		
	80	15.91		
	100	13.9		
100	20	597.4	597.4	20
	40	305.1		
	60	96.88		
	80	58.64		
	100	62.11		

4.3.1 Harvester Placed at $\frac{1}{4}$Th of the Bridge Length

Among the 5 velocity considerations, 40 mi/hr produces the maximum power for bridge length 25m at the first natural frequency of the bridge.Figure 4.2 shows the graph for this.

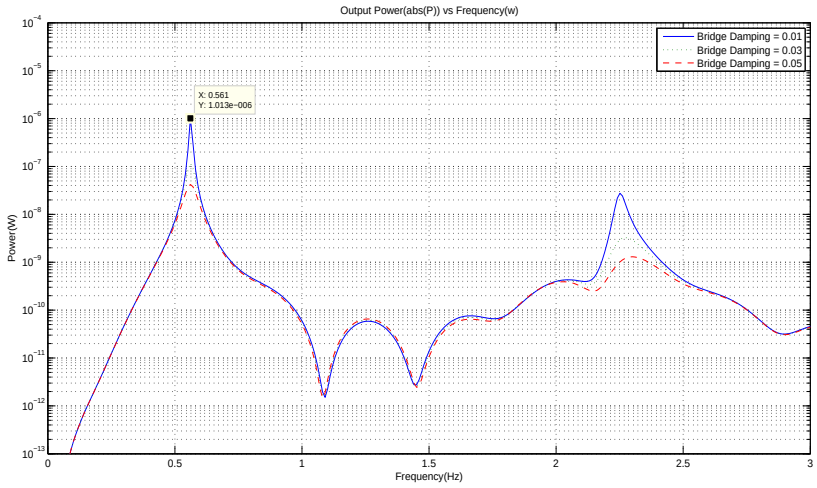

Figure 4.2: At velocity 40 mi/hr

Among the 5 velocity considerations, 20 mi/hr produces the maximum power for bridge length 50m at the first natural frequency of the bridge.Figure 4.3 shows the graph for this.

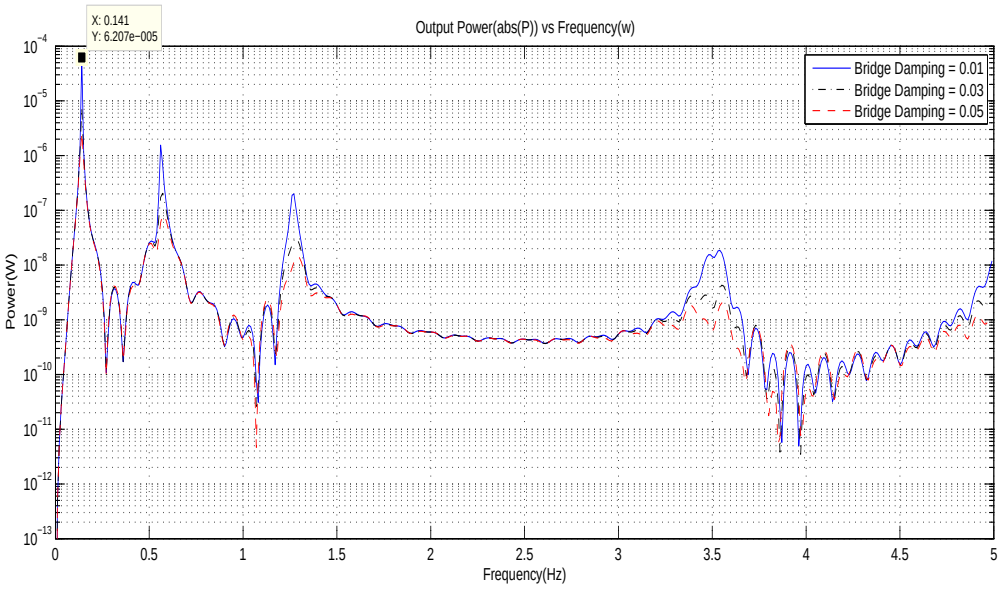

Figure 4.3: At velocity 20 mi/hr

Bridge length=75m

Among the 5 velocity considerations, 40 mi/hr produces the maximum power for bridge length 75m at the second natural frequency of the bridge.Figure 4.4 shows the graph for this.

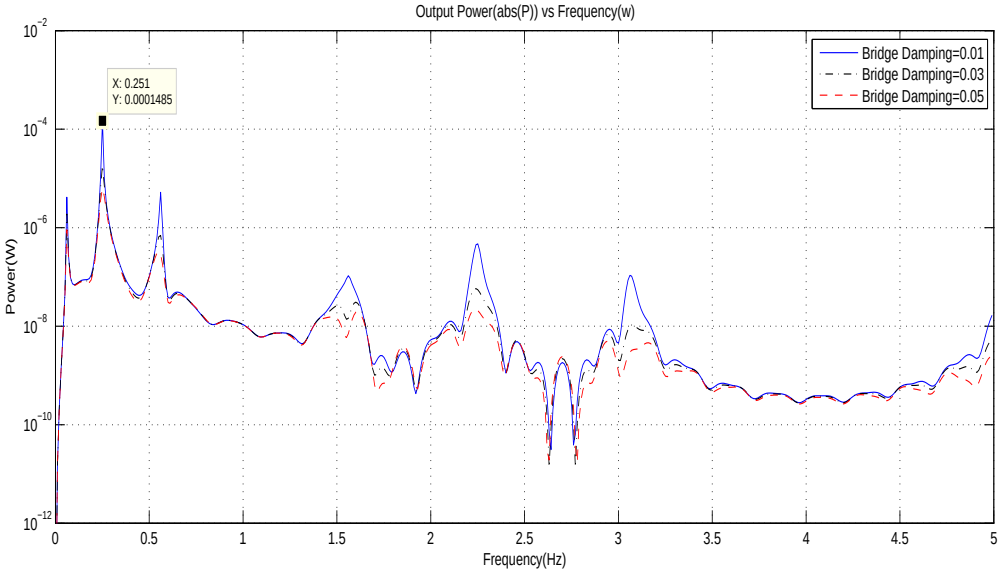

Figure 4.4: At velocity 40 mi/hr

Among the 5 velocity considerations, 20 mi/hr produces the maximum power for bridge length 100m at the second natural frequency of the bridge.Figure 4.5 shows the graph for this.

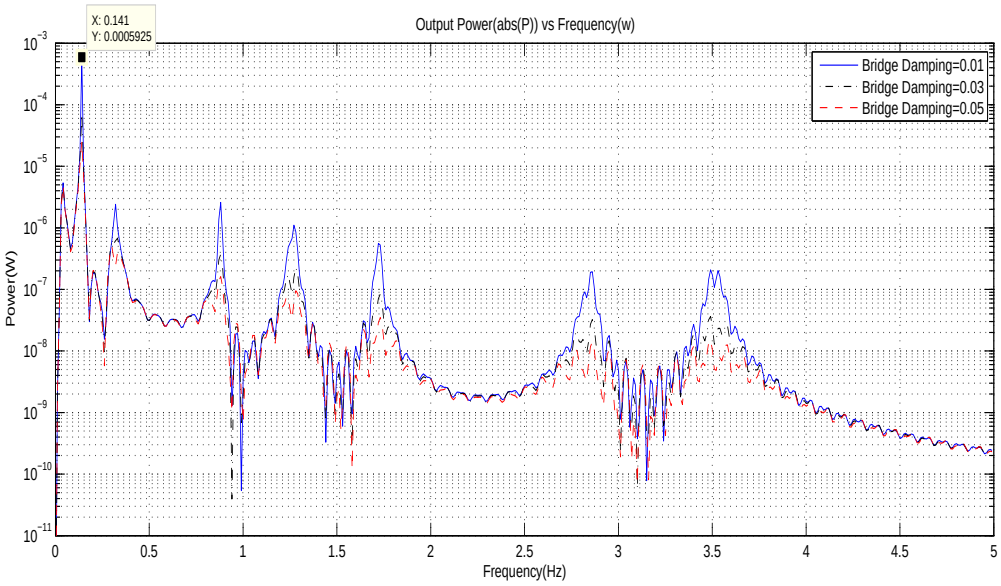

Figure 4.5: At velocity 20 mi/hr

4.3.2 Harvester Placed at $\frac{1}{2}$of the Bridge Length

Among the 5 velocity considerations, 40 mi/hr produces the maximum power for bridge length 25m at the first natural frequency of the bridge.Figure 4.6 shows the graph for this.

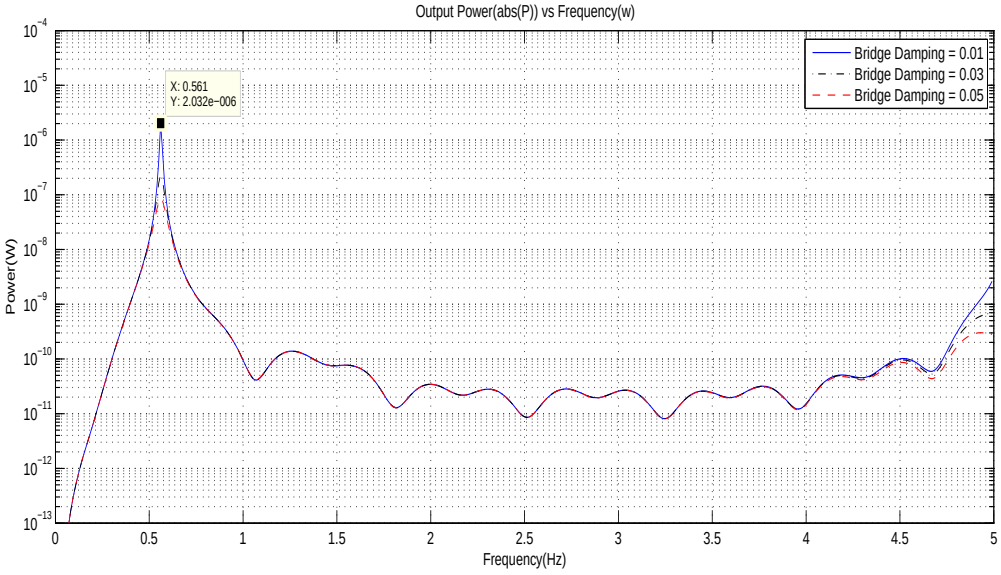

Figure 4.6: At velocity 40 mi/hr

Among the 5 velocity considerations, 20 mi/hr produces the maximum power for bridge length 50m at the first natural frequency of the bridge.Figure 4.7 shows the graph for this.

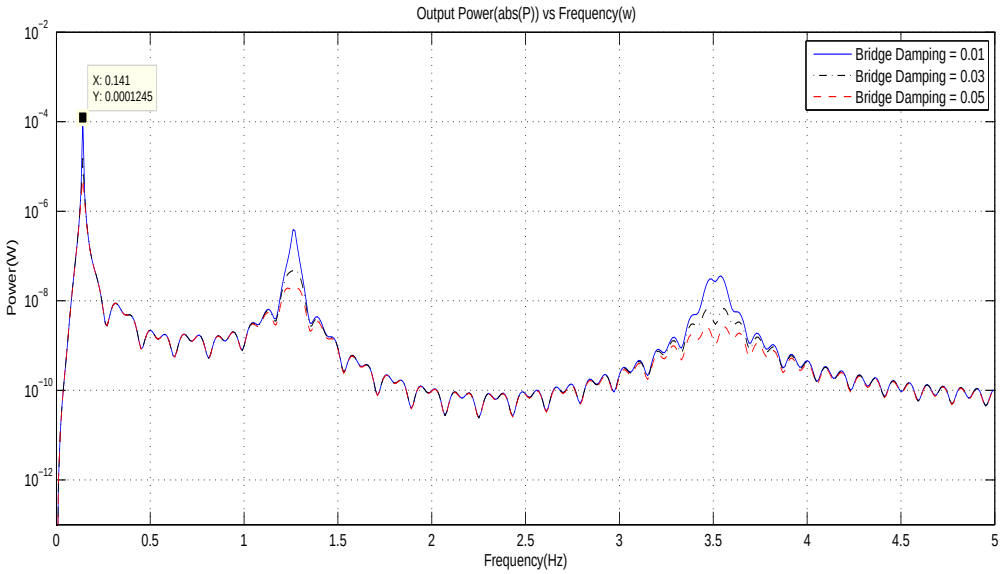

Figure 4.7: At 20 mi/hr

Among the 5 velocity considerations, 20 mi/hr produces the maximum power for bridge length 75m at the first natural frequency of the bridge.Figure 4.8 shows the graph for this.

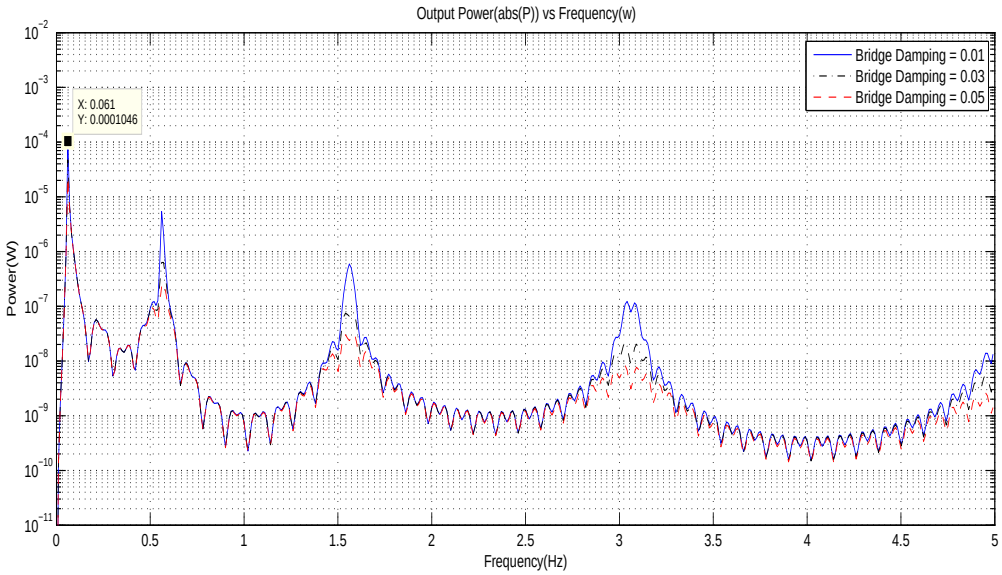

Figure 4.8: 20 mi/hr

Among the 5 velocity considerations, 40 mi/hr produces the maximum power for bridge length 100m at the fourth natural frequency of the bridge.Figure 4.9 shows the graph for this.

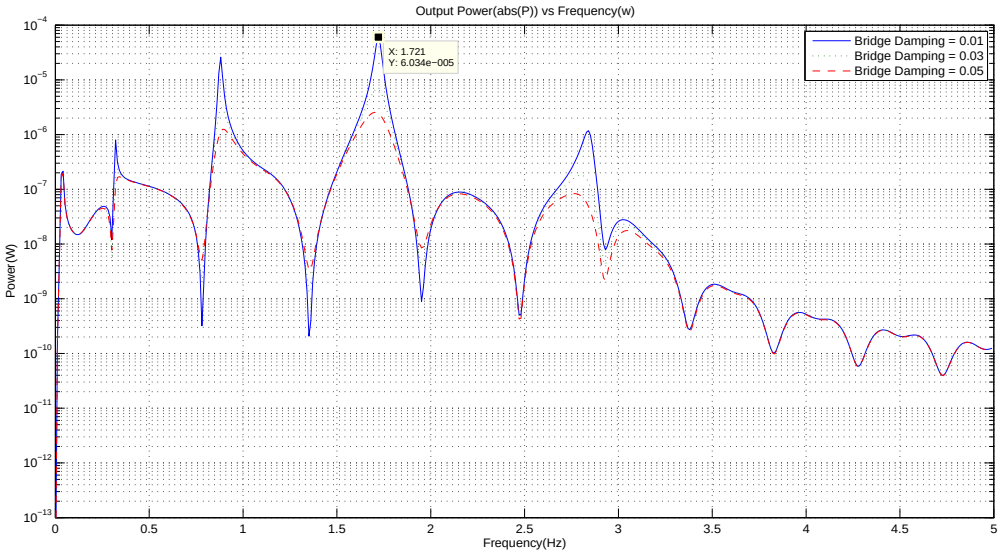

Figure 4.9: At velocity 40 mi/hr

4.3.3 Harvester Placed at $\frac{1}{4}$of the Bridge Length

Among the 5 velocity considerations, 40 mi/hr produces the maximum power for bridge length 25m at the first natural frequency of the bridge.Figure 4.10 shows the graph for this.

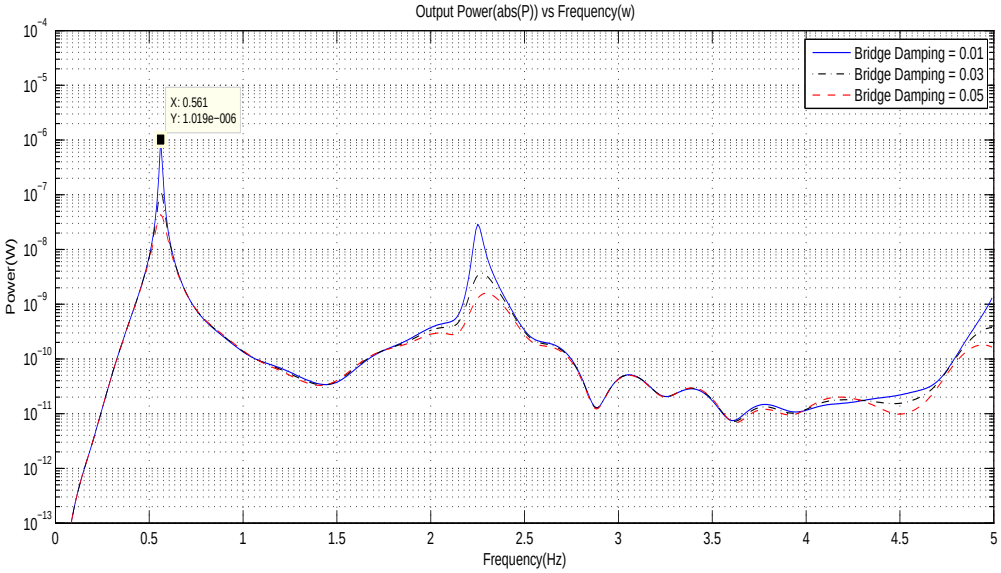

Figure 4.10: At velocity 40 mi/hr

Among the 5 velocity considerations, 20 mi/hr produces the maximum power for bridge length 50m at the first natural frequency of the bridge.Figure 4.11 shows the graph for this.

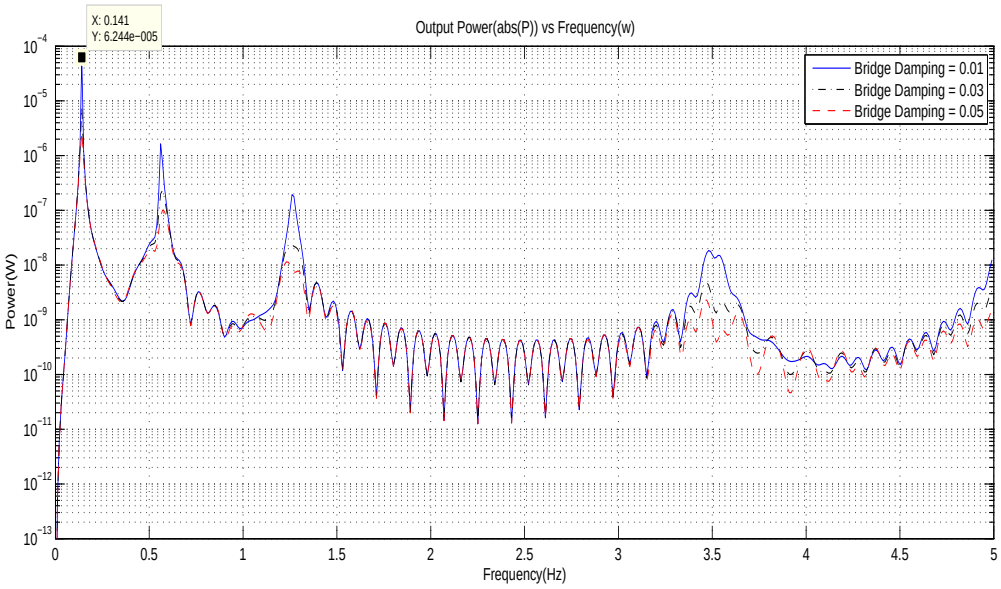

Figure 4.11: At velocity 20 mi/hr

Among the 5 velocity considerations, 40 mi/hr produces the maximum power for bridge length 75m at the first natural frequency of the bridge.Figure 4.12 shows the graph for this.

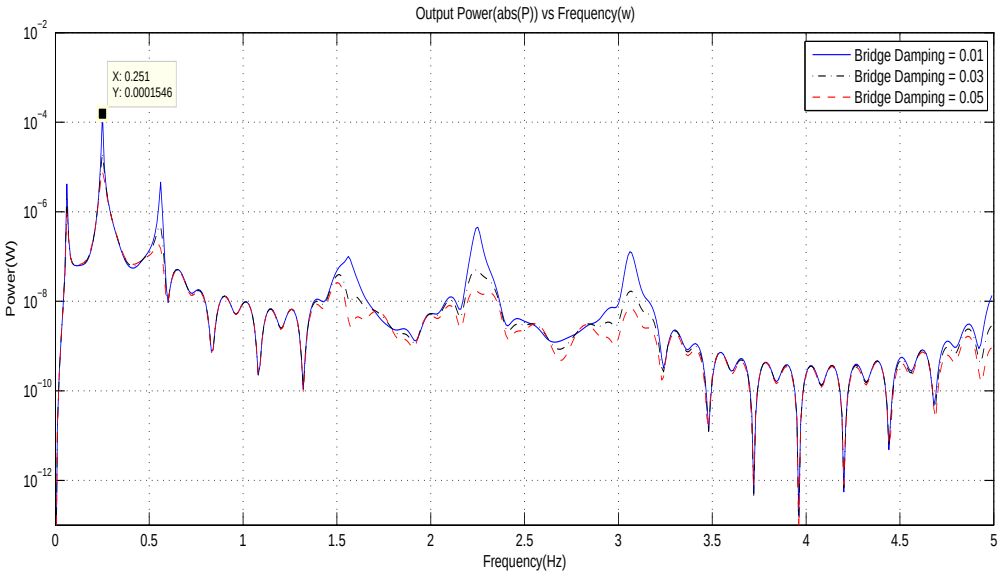

Figure 4.12: At velocity 40 mi/hr

Among the 5 velocity considerations, 20 mi/hr produces the maximum power for bridge length 100m at the first natural frequency of the bridge.Figure 4.13 shows the graph for this.

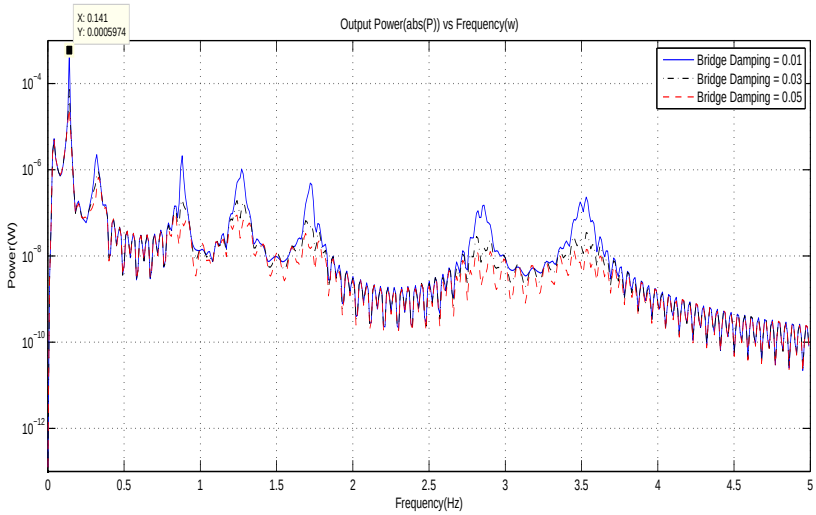

Figure 4.13: At velocity 20 mi/hr

4.4 Summary on Results

1. According to the results obtained,no single velocity can be specified for the maximum power generation. The maximum generated power occured either at $20mi/hr$ or $40mi/hr$ among the 5 velocity considerations:$20, 40, 60, 80$ and $100mi/hr$. For couple of cases the maximum power is seconded by the one at $60mi/hr$.

2. Bridge length of $75m$ and $100m$ turned out to be the most promising one as over a wide range of velocity the output power is good enough for powering small scale sensors.

3. Both the harvester location at $\frac{1}{4}$Th and $\frac{3}{4}$Th of the bridge length are found to be considered as potential application places for a considerable band width of velocities.

4. For each case, increasing the damping decreases the power production

5. Among all the possible cases considered here, the maximum power output is notified at the $\frac{3}{4}$Th of the bridge length when the bridge is of $100m$ length and under the moving load velocity $20mi/hr$.

Chapter 5

Discussion

From close scrutinizing of the generated MATLAB programme results(listed in previous chapter) the following points note worthy:

1. There are three distinct frequency very important in this problem contrast:(a)Bridge natural frequency,(b)Harvester natural frequency and (c) Excitation frequency(related to vehicle speed). To achieve higher efficiency, it is necessary to match the resonance frequency of the transducer with the most distinct frequency of the vibration source. Jeon et al. adjusted[21] various mechanical parameters, including the resonant frequency and the location of a harvester, to maximize the strain induced in the piezoelectric element in order to improve power output. The power generation was increased by a factor of 25 when the frequency of the harvesting device was well tuned to that of the structure. Roundy and Wright[9] also suggested that the harvesting system should be designed such that the harvester could be excited at its resonance. The proof mass is usually used to maximize the power output. The vibration present in a structure is, however, usually much lower than the resonance of a harvesting device and often changes during operation; therefore, this vibration does not always effectively couple energy to the harvester. The optimization of the transducer setup and geometry is one of the most challenging tasks during the design, but it has received less attention from researchers.

2. The harvester material natural frequency is cautiously chosen to be low so as to close to that of bridge first natural frequency. As described in the previous point, it enhances the possibility of picking up the usual maximum deflection of the bridge successfully and hence producing usu able power. Bearing this is in mind, it is interesting to note that, the pick powers are generated at the natural modes of the bridge only, not at the harvester one. It may be paraphrased as, if the harvester material is chosen such that its fundamental natural mode is close to the bridge fundamental natural frequency, then from different vehicle speed maximum power can be located at the bridge mode frequencies only.

3. At slower vehicle speed, in the power generation graph, more picks and valleys are notified than the higher speeds. It is well expected as the vehicle moves slower, it gets more time to interact with the bridge and so the response is also more.

4. Whenever a vehicle moves on a bridge, theoretically,it excites infinite number of modes of the bridge.But the considerable amount of excitation generally comes from the first few mode shapes and more precisely the major contribution from the first mode shape irrespective of the speed. As the speed goes up, more modes with considerable amount of excitations are noted.

5. Naturally, with a longer span length the first natural mode shape frequency of the bridge becomes smaller than that of its shorter counter part and there are more possibilities of promising excitation of more than one bridge mode shapes arise.

6. The harvester is considered at 3 distinct places along the bridge span length. Also, for every velocity of the vehicle, the deflection is calculated for the first 10 natural frequencies corresponding to the first 10 mode shapes of the bridge. In other words, the deflection calculated is the summation of the contribution from different mode shapes of the bridge. The consequence is that the same place which is deflected for one mode shape in a certain direction and hence a promising candidate for the energy harvesting purpose may have an opposite deflection for some other mode shape at the same place and hence nullify the advantage of greater deflection in first case.

Chapter 6

Conclusion

This thesis was conducted with a focus on exploring the qualitative nature of the bridge dynamics interaction with the piezoelectric energy harvester. A simply supported beam with a constant moving load was considered for the bridge dynamics while the piezoelectric energy harvester was represented with a 1D model. Later on, physical sytems for the bridge and the energy harvester were adopted from two disticnt research and coupled together under the developed model. Different velocity, bridge length and harvester location on the bridge are monitored. The maximum power($0.6\mu W$) is obtained at $\frac{3}{4}$Th of the bridge length when the bridge is of $100m$ length and under a constant moving load of $1000N$ at a speed of $20mi/hr$.This power is not sufficient enough to meet power consumption requirements of different components of a structural health monitoring sytem(Reference values can be found at Table 1.1). But if only power requirement for data tranmission is taken into consideration, theoretically, this power is capable of sending Radio frequency data at $30m$ distance per $4s$(Reference to Table(1.2)), provided the above mentioned moving load conditions are mentained.

Chapter 7

Further recommendation

1. In this thesis, Bridge dynamics is modelled as a simply supported beam with a constant load moving on it. This simplification is good enough for the first approach.But the practicality does not resemble so. Next step should be considering the vehicle dynamics of the simplest form with a moving mass and spring. A more complexity can be added later on by considering different vehicle dynamics and hence leading to a complete understanding of the whole scenario.

2. The efficiency of the power harvesting circuitry must be maximized to allow the full amount of energy generated to be transferred to the storage medium. The continuous advances that are being made in low power electronics must be studied and utilized to both optimize power flow from the piezoelectric and minimize circuit losses. Gains in this area are a necessity for the successful use of piezoelectric materials as power harvesting devices.The thesis was modelled with a single resistence load. An inductor circuit consideration opens up much flexibility over the generated power management.

3. The major limitations facing researchers in the field of power harvesting revolve around the fact that the power generated by piezoelectric materials is far too small to power most electronics. Therefore, methods of increasing the amount of energy generated by the power harvesting device or developing new and innovative methods of accumulating the energy are the key technologies that will allow power harvesting to become a source of power for portable electronics and wireless sensors.

4. Last but not the least, experimental set up is a necessity to verify any kind of theoretical outcome.

Bibliography

[1] Fryba,L., *Vibration of Solids and Structures under Moving Loads.* Thomas Telford,London,UK,1999.

[2] duToit N E and Wardle B L , Experimental Verification of models for microfabricated piezoelectric vibration energy harvesters *AIAA J.* 2007 45, pp 1126-37

[3] Sodano, H. A. & Park, G. & Inman, D. J. Estimation of Electric Charge Output for Piezoelectric Energy Harvesting. *Strain* 2004 40,pp 49-58

[4] Celebi, M. Seismic Instrumentation of Buildings (with Emphasis of Federal Buildings) *Technical Report No. 0-7460-68170.*United States Geological Survey, Menlo Park, CA, USA,2002 .

[5] Farrar, C. R. Historical Overview of Structural Health Monitoring. *Lecture Notes on Structural Health Monitoring Using Statistical Pattern Recognition* Los Alamos Dynamics, Los Alamos, NM, USA,2005.

[6] Nagayama, T. Structural Health Monitoring Using Smart Sensors. *Ph. D. Dissertation* University of Illinois at Urbana-Champaign, Urbana, IL, USA,2005 .

[7] Chiu, Y., & Tseng, V. F. G. Capacitive Vibration-to-electricity Energy Converter with Integrated Mechanical Switches. *in Proc. PowerMEMS 2007* ,pp 121–124.

[8] Despesse, G., Jager, T., Basrour, S., Chaillout, J. J., Charlot, B., Léger, J. M., et al. A Fabrication and characterization of high damping electrostatic micro devices for vibration energy scavenging. *in Proc. Design, Test, Integration and Packaging of MEMS and MOEMS (DTIP'05)* 2005.

[9] Roundy, S., Wright, P. K., & Rabaey, J. A study of low level vibrations as a power source for wireless sensor nodes. *Comp. Com.* 2001 26, 1131–1144.

[10] Sterken, T., Fiorini, P., Baert, K., Puers, R., & Borghs, G. An electret-based electrostatic μ-generator. *in Proc. International Conference on Solid-State Sensors, Actuators and Microsystems (TRANSDUCERS '03)* 2003, pp 1291-1294

[11] Sterken, T., Fiorini, P., Baert, K., Borghs, G., & Puers, R. Novel design and fabrication of a MEMS electrostatic vibration scavenger. *in Proc. PowerMEMS* 2004

[12] Miao, P., Mitcheson, P. D., Holmes, A. S., Yeatman, E. M., Green, T. C., & Stark, B. H. *Mems inertial power generators for biomedical applications. Microsystem Technologies* 2006 12, pp 1079– 1083.

[13] Meninger, S., Mur-Miranda, J. O., Amirtharajah, R., Chandrakasan, A. P., & Lang, J. H. Vibration-to-electric energy conversion. *IEEE VLSI Syst.* 2001 9, pp 64–76.

[14] Lim, P., Basset, P., Paracha, A. M., Marty, F., Poulichet, P., & Bourouina, T. Design and fabrication of a novel electrostatic MEMS-based vibration-to-electric energy converter based on parallel plates with in-plane mechanism *in Proc. Asia- Pacific Conference of Transducers and Micro-Nano Technology (APCOT)* 2006.

[15] Paracha, A. M., Basset, P., Marty, F., Chasin, A. V., Poulichet, P., & Bourouina, T. A high power density electrostatic vibration-to-electric energy converter based on an in-plane overlap plate (IPOP) mechanism. *in Proc. Design, Test, Integration and Packaging of MEMS and MOEMS (DTIP'07)* 2007.

[16] Ching,N. N. H. , Chan,G. M. H. Li,W. J. Wong,H. Y. and Leong,P. H. W. Pcb integrated micro generator for wireless systems. *in Intl. Symp. on Smart Structures and Microsystems* October 2000, pp 19-21

[17] Veld,B.O. ,Hohlfeld, D. & Pop,V. Harvesting mechanical energy for ambient intelligent devices. *Inf Syst Front* 2009 11,pp 7–18.

[18] Lynch,Jerome P. and Loh,Kenneth J. A Summary Review of Wireless Sensors and Sensor Networks for Structural Health Monitoring. *The Shock and Vibration Digest* 2006 38, 91

[20] Mateu,L. and Moll,F. Review of Energy Harvesting Techniques and Applications for Microelectronics. *Proceedings of the SPIE Microtechnologies for the New Millenium* 2005

[21] Jeon, Y. B., Sood, R., Jeong, J. H., & Kim, S. G. MEMS power generator with transverse mode thin film PZT. *Sens. Act. A.* 2005, 122,pp 16–22.

[22] http://www.scsolutions.com/public/research/projects/668-DSY.html

[23] Glynne-Jones, P., Beeby, S. P., & White, N. M. Towards a piezoelectric vibration-powered microgenerator. *IEE Proceedings* Science Measurement and Technology 2001,148, pp 68–72.

[24] Goldschmidtböing, F., Müller, B., & Woias, P. Optimization of resonant mechanical harvesters in piezopolymer-composite technology. *in Proc. PowerMEMS* 2007, pp 49–52.

[25] http://www.physikinstrumente.com/en/products/piezo_tutorial_introduction.php

[26] Vives, A. A. *Piezoelectric Transducers and Applications.* Springer Berlin Heidelberg, Berlin, Germany, 2008.

[27] duToit,N.E. Modeling and Design of a MEMS Piezoelectric Vibration Energy Harvester.*MSc Thesis* Massachusetts Institute of Technology, USA,2005

[28] Kreiszig,E. *Advanced Engineering Mathematics.* Jhon Wiley and Sons Inc ,U.S.A.,2006

[29] Yang,Y.B.,Lin,C.W. & Yau,J.D. Extracting bridge frequencies fromthe dynamic response of a passing vehicle. *Journal of Sound and Vibration* 2004,272,pp 471–493

[30] Kendall,C.J. Parasitic Power Collection in Shoe Mounted Devices. *BSc Thesis* Massachusetts Institute of Technology, USA,1998

[31] Kim,S.,Pakzad,S.,Culler,D.,Demmel,J.,Fenves,G.,Glaser,S. & Turon,M. Health Monitoring of Civil Infrastructures Using Wireless Sensor Networks. *IPSN'07* 2007, Cambridge, Massachusetts, USA.